An Investigation of the Role of Enzyme Phosphopantetheinyl Hydrolase in *Mycobacteria*

Honors Thesis

Presented to the College of Agriculture and Life Sciences,

Cornell University

in Partial Fulfillment of the Requirements for the

Biological Sciences Honors Program

by

Annie M. Geiger

May 2019

Dr. Carl F. Nathan

Dr. David Russell

Abstract

Phosphopantetheinyl transferase (PptT) is an essential enzyme in *Mycobacterium tuberculosis* (Mtb) that adds a pantothenate group onto carrier proteins using coenzyme A (CoA), changing them from the apo to holo enzyme configuration. Encoded for in the same operon, phosphopantetheinyl hydrolase (PptH) is a newly identified enzyme that counterbalances this reaction by removing the pantetheine group from the holo-carrier protein, resulting in an apo-carrier protein. Because PptH appears to operate a futile cycle in the cell, its purpose remains unknown. In this project, I aimed to understand the functions of PptH and the conditions in which it becomes essential in the mycobacterial cell through a series of chemical stress tests and an analysis of binding partners of PptH. Select chemical stress growth assays indicated that *Mycobacterium smegmati*s (Msm) strains encoding putative PptH loss-of-function (LOF) mutations possess impaired cell wall integrity. CRISPRi was used to test for synthetic lethality in the proposed role of PptH in a CoA salvage pathway. Co-IPs were not able to show that PptH and its neighboring enzyme, PptT are binding partners. These results glean insight into mycobacterial biology, the functions of PptH, and its efficacy as a putative drug target for tuberculosis.

List of Common Abbreviations:

ATc (Anhydrotetracycline)

ACP (Acyl carrier protein)

CoA (Coenzyme A)

Comp (Complement)

CRISPRi (CRISPR interference)

IP (Immunoprecipitation)

kd (Knockdown)

k/o (Knockout)

LOD (Limit of Detection)

LOF (Loss-of-Function)

MIC (Minimum Inhibitory Concentration)

Msm (*Mycobacterium smegmatis*)

Mtb (*Mycobacterium tuberculosis*)

OD (Optical Density)

PAM (Protospacer adjacent motif)

PBS (Phosphate-Buffered Saline)

Ppt (Phosphopantetheine)

PptH (Phosphopantetheinyl hydrolase)

PptT (Phosphopantetheinyl transferase)

SDS (Sodium Dodecyl Sulfate)

Tet (Tetracycline)

TB (Tuberculosis)

ZOI (Zone of Inhibition)

8918 (1-[(2,6-diethylphenyl)-3-N-ethylcarbamimodoyl] urea)

Introduction

Nearly one quarter of the world's population is believed to be latently infected with *Mycobacterium tuberculosis* (Mtb) and tuberculosis (TB) is the primary driver of mortality from infectious disease (Houben & Dodd, 2016; "Tuberculosis (TB)," 2017). Mtb is inhaled in the form of aerosol droplets, where once established in the lungs, is consumed by macrophages that can distribute the bacteria throughout the body. The host immune system often responds by isolating Mtb in granulomas, where the bacteria are non-replicating and may remain dormant indefinitely. These people, who are latently infected with TB, are therefore asymptomatic and not infectious. Those whose immune system does not effectively contain the infection may experience a reactivation of Mtb, and the bacilli can spread to other organs (Barry et al., 2009). Risk factors for TB include conditions that are immunocompromising, such as diabetes and HIV/AIDS. Malnourishment resulting from excessive alcohol and non-injectable drug use, as well as homelessness, or residence in a correctional facility can also increase risk for TB infection ("Tuberculosis (TB)," 2018).

The current drug regimen to treat tuberculosis involves six months of multi-drug antibiotic therapy, consisting of two months of daily treatment with rifampicin (RIF), pyrazinamide, ethambutol, and isoniazid (INH), followed by four months of daily treatment with RIF and INH (World Health Organization, 2010). However, many of the countries with the highest rates of TB lack the health infrastructure required for timely diagnosis, and people with the disease may not be able to secure a steady supply of drugs. Often, the full course of antibiotics is not completed due to a lack of consistent healthcare access, the early disappearance

of symptoms, or unpleasant side effects. As a result, emerging resistance to the standard drug regimen has become a major global problem, with 500,000 new cases of multidrug-resistant (MDR) and extensively drug-resistant (XDR) TB in 2016 reported by the CDC ("Tuberculosis (TB)," 2018). Drug-resistant TB can take up to 32 months to treat, and reduces the successful patient treatment rate to 50% (World Health Organization, 2010). There is a global need for new drug targets, as Mtb evolves resistance to current drugs.

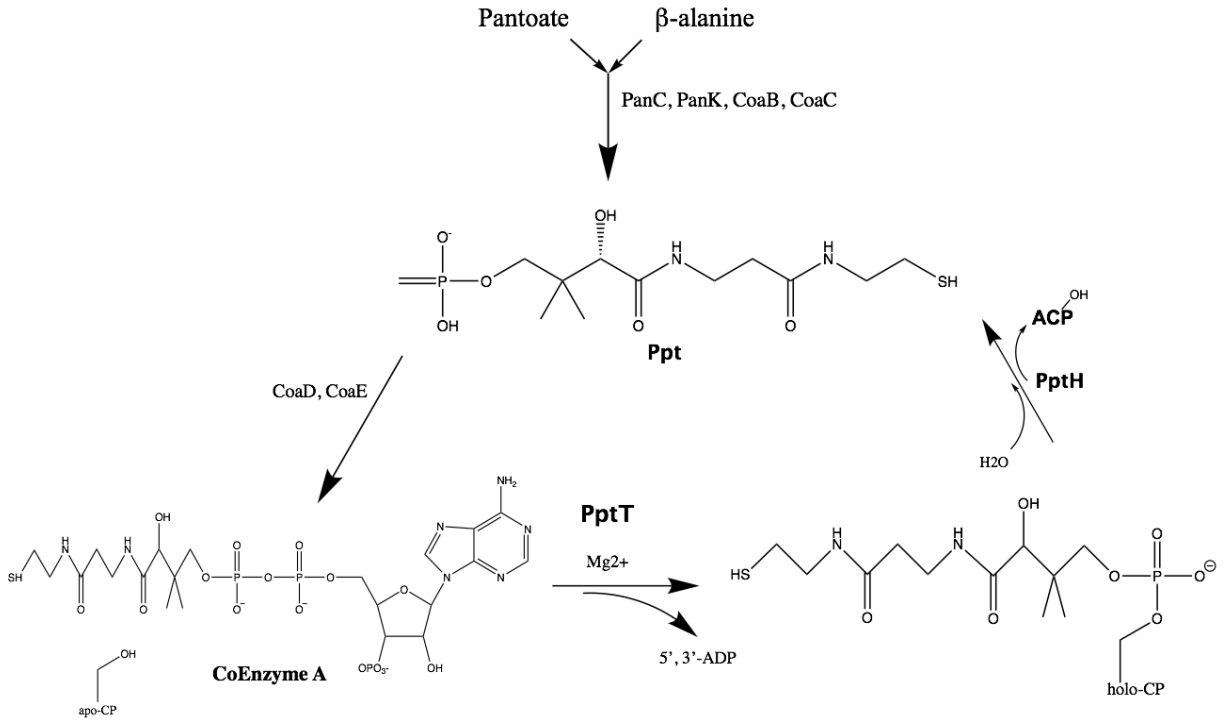

Fig. 1. PptT and PptH reaction mechanism. PptT removes Ppt from coenzyme A (CoA) and covalently attaches this group onto acyl carrier proteins (ACPs) (figure adapted from LeBlanc et al., 2012, Ballinger, 2018, and Nathan, 2018). PptH catalyzes the conversion of holo-ACPs to apo-ACPs through the removal of Ppt. The putative role of PptH in a CoA salvage pathway is shown: while forming apo-ACPs, PptH releases Ppt, which is required for the synthesis of CoA.

Phosphopantetheinyl transferase (PptT) is currently under exploration as a drug target in Mtb and no drug-like inhibitors of PptT are known. In Mtb, *rv2794c* encodes for PptT, which charges ACPs for the synthesis of key structural lipids. PptT transfers a 4′-phosphopantetheine group onto carrier proteins such as polyketide synthases and fatty acid synthases using coenzyme A (CoA), changing them from the apo to holo enzyme configuration (Fig.1). This enzyme is essential in Mtb and the reaction it catalyzes is involved in the production of long-chain fatty acid cell wall lipids such as mycolic acids, and lipids that serve as virulence factors such as phthiocerol dimycocerosates (PDIMs) that modulate host immune reactions. PptT also catalyzes the biosynthesis of mycobactins that act as siderophores. Because the intrinsic drug resistance of Mtb is tied to its unusual, lipid-rich cell wall, PptT is an attractive drug target (LeBlanc et al., 2012).

PptT is the target of an amidino-urea compound identified in a high throughput screen with Sanofi, a collaborating pharmaceutical company. This mycobactericidal compound, named 8918, inhibits PptT by binding in its active site. The structure of 8918 is shown below in Fig. 2. The minimum inhibitory concentration for 90% of bacterial growth (MIC_{90}) of 8918 against H37Rv Mtb, a laboratory strain that is virulent in a mouse model, was determined to be 3.1 mM (Ballinger et al., 2019). Elaine Ballinger identified mutant Mtb colonies resistant to 8918. The majority of these mutants had a resistance conferring mutation that was a putative loss-of-function (LOF) in the neighboring gene *rv2795c*, encoding the enzyme phosphopantetheinyl hydrolase (PptH). Further analysis of this enzyme elucidated a novel mechanism of resistance in *Mycobacteria*. Some resistant mutants also had mutations in *pptT*, although these mutations were rarer (Ballinger, 2018).

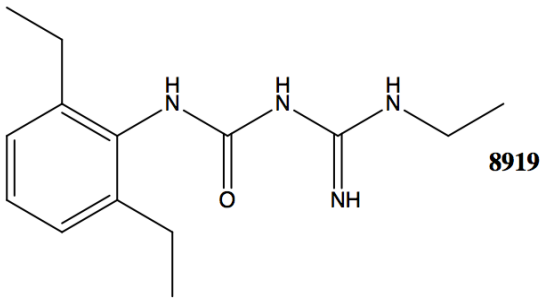

Fig. 2. **Structure of 8918 (1-[(2,6-diethylphenyl)-3-N-ethylcarbamimodoyl] urea)**: A mycobactericidal compound that targets PptT by binding in the Ppt binding site (figure adapted from Ballinger et al., 2019).

Encoded for by *rv2795c* in Mtb, PptH is a metallophosphoesterase that removes the Ppt group from the holo-carrier proteins, resulting in apo-carrier proteins. PptH appears to counterbalance the activities of PptT, and operate a futile cycle as it has no obvious utility to the cell. Unlike PptT, PptH is not known to be essential to the cell under any conditions. This enzyme is similar in function to non-homologous acyl carrier protein (ACP) hydrolases, but was named PptH by the Nathan laboratory as it is a newly identified enzyme in Mtb. Like PptH, ACP hydrolases remove Ppt from ACPs in vitro, as demonstrated in Fig. 1 (Ballinger et al., 2019). Also similar to PptH, ACP hydrolase in *E. coli* performs hydrolysis and utilizes magnesium, although the two enzymes are not structurally homologous (Ballinger, 2018). The enzyme is highly conserved in *Mycobacteria*, as orthologous genes to *rv2795c* exist in *M. smegmatis* (Msm), *M. leprae, M. bovis*, and *M. marinum* (Mycobrowser, 2018). The retention of PptH in *M. leprae* is noteworthy, as the genome of this species is highly reduced, thus implying a significant function for PptH (Ballinger et al., 2019).

In this report, I aimed to understand the conditions in which PptH becomes essential so as to determine its physiological functions. Because LOF of PptH leads to resistance to PptT

inhibitor compound 8918 and PptT is involved in cell wall formation, I hypothesized that PptH may be involved in cell wall integrity. To test cell wall viability, I designed a series of stress tests with chemicals known to target the mycobacterial cell wall or represent the conditions that Mtb encounters in the human macrophage. Chemical stress tests were completed with wild type (WT) and putative PptH LOF mutant Msm strains. Msm is a fast-growing species of *Mycobacteria* that is non-pathogenic to humans.

Beyond involvement in cell wall integrity, I hypothesized that PptH was involved in a CoA salvage pathway, as elucidated in Fig. 1. By removing the phosphopantetheine group from holo-carrier proteins, PptH activity releases free pools of Ppt, which is the precursor for Coenzyme A. It may be energetically advantageous for the cell to not be required to synthesize Ppt *de novo* from pantoate and beta-alanine, and so PptH may operate a CoA salvage path. I designed CRISPRi ATc-regulated knockdowns of two essential enzymes in the synthesis of Ppt to test for synthetic lethality in PptH LOF mutant cells, which would indicate the role of PptH in a CoA salvage pathway. These enzymes were pantothenate B (*panB*) and pantothenate C (*panC*), which are essential enzymes involved in synthesizing pantothenate in the first steps of the CoA biosynthesis pathway.

Because the function of PptH is not fully characterized, I aimed to additionally find the binding partners, modifications, and substrates of PptT and PptH. Because PptT and PptH are encoded for by adjacent genes in the same operon, I hypothesized that they may be binding partners because they are co-transcribed. Their relationship within the same pathway means that their interaction is possible, although this interaction may be transient. Co-immunoprecipitations (Co-IPs) were conducted to detect putative binding interactions between the two proteins. Prior

to conducting Co-IPs, protein detection methods were optimized through determining antibody detection limits, western blotting, and antibody purification protocols.

Materials and Methods

Strains of Msm: *M. smegmatis* mc^2155 WT,

M. smegmatis mc^2155 D161E, Y97D, -AA23-25, H246N} these are all putative LOF PptH mutants resistant to 8918.

Sequences of WT PptH and putative LOF mutant PptH are shown in Fig. S1.

Strains of Mtb: *M. tuberculosis* H37Rv, *rv2795c* knockout (published in Ballinger et al., 2019), complement (unpublished), H246N (unpublished)

Growth media:

Liquid: Middlebrook 7H9 complete: contains tyloxapol, glycerol and ADN (NaCl, Albumin Fraction V, Dextrose)

Solid: Middlebrook 7H11, glycerol and Middlebrook OADC Enrichment (Oleic acid, Albumin Fraction V, Dextrose, and Catalase)

8918 MIC Assay:

Msm strains were grown to log phase in 7H9 and diluted to an OD600 of 0.1 in 7H9. 200 μL of culture were added to each well of a 96-well plate, and 2 μL of 8918 was added to each well in a 2-fold dose response. Moxifloxacin was used as a control in the same method as above, with 2-fold dose response dilutions across the plate from 1 ng/ml to 1 μg/ml. The OD600 of the plate was read after 2 days of incubation at 37°C. Results are shown in Fig S2.

Confirmation of mutations in *rv2795c*: Genomic DNA was extracted from Msm strains and *rv2795c* was amplified using primers flanking the gene (provided in Table 1). Polymerase chain

reaction (PCR) products were run on agarose gels, gel purified, and sent for sequencing to confirm mutations. Sequences were analyzed using the ExPASY and Multalin programs and results are shown in Fig. S1.

Primer location	Forward Primer	Reverse Primer
Middle of *rv2795c*	5'ATGTTCCTGCTGTACGACTAC3'	5'CCACGATGTTGCGTTCCTTGG3'
3' end of *rv2795c*	5'CTGGACGGTTATCCGTTCGAG3'	5'CGGCAGAACCAGGGAAAGCAG3'

Table 1. **Primers for sequencing *rv2795c* mutations.** Primers used to sequence Msm putative PptH LOF mutants and the WT strain were designed to contain about fifty percent G-C content.

Structural modeling of PptH mutants: Phyre and PyMol computer programs were used to predict the location of mutations in relation to the active site. Surface cavity detection was set to a radius of 4 solvent radii.

Growth curves: Msm cultures were grown to log phase in 7H9 and diluted to an OD600 of 0.1 in 7H9. 200µl of culture at an OD600 of 0.1 was loaded into each well of a 96-well plate to begin. Data was collected with a Spark machine. Machine conditions were shaking at 27°C, with an OD600 measurement taken automatically every hour for 48 hours. The OD measurement for each well was the average of five, one in each quadrant of the well and one in the center.

Chemical Stress Tests: For all chemical stress treatments, experiments were performed in duplicate and 7H9 was used as a control for the chemical unless otherwise indicated. OD was read using a spectrophotometer. Msm WT, D161E, Y97D, and –AA23-25 were used for each test and technical replicates of each sample were made in triplicate. For all tests that involved

plating, an input cell count was obtained by removing culture aliquots before the chemical was first added on Day 0, diluting serially in PBS, and plating on 7H11.

Phosphate buffered saline (PBS) PBS-1% tyloxapol treatment of Msm strains, and Msm WT with 3 μM 8918: Cells were grown in 7H9 in 50 ml polystyrene tubes to log phase, pelleted and washed twice in PBS-1% tyloxapol before being resuspended to an OD600 of 0.1 in PBS-1% tyloxapol. Cultures were shaken for 48 hours at 37°C, then diluted serially in ten-fold and spot-plated on 7H11 growth media in triplicate. 10 μl of culture was plated for each spot. Cultures were shaken for 6 more days at 37°C, and were then diluted serially and plated on 7H11 growth media in the same method. Plates were incubated for 2 days at 37°C, after which colonies were counted.

Acidified sodium nitrite (3 mM and 6 mM) treatment of Msm strains and Msm WT with 3 μM 8918 with either 3 mM or 6 mM $NaNO_2$ diluted from a 100 mM stock of pH 4. Acidified 7H9 at pH 5.5 functioned as a control for the effects of sodium nitrite. Cells were grown in 7H9 in 50 ml polystyrene tubes to log phase, pelleted and washed twice in PBS-1% tyloxapol before being resuspended in 3 mM or 6 mM NaNO2 or pH 5.5 7H9 in 96 well plates with a starting OD600 of 0.1. Cultures were incubated for 5 days at 37°C, diluted serially in PBS, and then plated on 7H11. Plates were incubated for 2 days at 37°C, and then colonies were counted. The duration of time for exposure to and recommended concentrations of $NaNO_2$ for experimental use were detailed previously (Darwin & Nathan, 2005).

Osmotic treatment of Msm strains and Msm WT with 3 μM 8918 through exposure to water or 0.5 M NaCl: Cells were grown in 7H9 in 50 ml polystyrene tubes to log phase, pelleted and washed twice in PBS-1% tyloxapol before being resuspended in water or 0.5 M NaCl to an OD580 of 0.1. Cultures were shaken for 4 hours at 37°C, then diluted serially and plated on

7H11 growth media. Plates were incubated for 2 days at 37°C, and then colonies were counted. Duration of exposure as well as experimental chemical concentrations were adapted from (Gebhard, Humpel, Mclellan & Cook, 2008).

SDS liquid treatment of Msm strains and Msm WT with 3 μM 8918 strains: Cells were grown in 7H9 in 50 ml polystyrene tubes to log phase, pelleted and washed twice in PBS-1% tyloxapol before being resuspended in 0.5% or 0.05% SDS. Cultures were shaken for 4 hours at 37°C, then diluted serially and plated on 7H11 growth media. Plates were incubated for 2 days at 37°C, and then colonies were counted. Experimental chemical concentrations and duration of chemical exposure time were found in (White et al., 2010; Manganelli, Voskuil, Schoolnik & Smith, 2001).

SDS stress in plates: Msm cells were grown in 7H9 in 50 ml polystyrene tubes to log phase, pelleted and washed twice in PBS 1% tyloxapol, then resuspended in PBS to an OD580 of 0.1. Cultures were serially diluted in PBS and then plated on 7H11 plates containing 0.00375%, 0.005%, or 0.0075% SDS. Plates were incubated for 2 days at 37°C, and then colonies were counted. This alternative SDS exposure experimental protocol was adapted from (Daugherty, Powers, Standley, Kim & Purdy, 2011).

Lysozyme MIC for Msm strains in 96-well plates: Cells were grown in 7H9 in 50 ml polystyrene tubes to log phase, pelleted and washed twice in PBS-1% tyloxapol. 200 μl of OD600 0.02 was added to each well in a 96-well plate. A drug plate was created with lysozyme diluted in triplicate two-fold across the plate in 7H9, starting at a concentration of 40 mg/ml, diluted down to 0.156 mg/ml. Moxifloxacin diluted in DMSO in triplicate was used as a control, with two fold dilutions across the plate from 3 μg/ml to 0.01 μg/ml. 2 μl from each drug well was diluted 1:100 into each well containing culture and plates were incubated for 3 days at 37°C.

OD was read with a spectrophotometer. Suggested concentrations for lysozyme were retrieved from (Flores, Parsons & Pavelka, 2005).

EtBr uptake assay to measure cell membrane permeability: Msm cells were grown to log phase in 7H9, washed in 1X PBS/Tween80, and diluted to an OD600 of 0.8 with 0.4% glucose. 100 µl of cells at an OD600 of 0.4 was added in triplicate to a 96-well plate on ice. 8 µg/ml of EtBr in 1X PBS/Tween80-0.4% glucose was prepared and added in 100 µl aliquots to the culture wells, to achieve a final concentration of 4 µg/ml EtBr. An excitation value of 530 nm and emission value of 590 nm were used to detect fluorescence, which was read every minute for one hour. 1X PBS/Tween80-0.4% glucose was used as a control. A SpectraMax microplate reader was used to measure OD. This protocol was adapted from Kristin Burns-Huang.

CRISPRi cloning was utilized to generate two pantothenate B (*panB*) and pantothenate C (*panC*) knockdown targeting strains in Msm WT and strains D161E and -AA23-25. These are two essential enzymes in the synthesis of Ppt. The protospacer adjacent motif (PAM) sequences chosen for the knockdowns were of varying strengths, with *panC1* possessing the greatest fold knockdown ability described, *panB1* at half of this level, and *panC2* and *panB2* at 43% and 35% of the recorded knockdown ability of *panB1*, respectively (Table 2). A non-targeting control sequence was also created for each enzyme to use as a negative control. An anhydrotetracycline (ATc)-inducible sgRNA was used to prevent transcription of these enzymes in the presence of ATc. The Msm CRISPRi plasmid backbone pLJR692 was used, which carries a kanamycin resistance cassette (Rock, 2017).

The pLJR692 plasmid was digested with restriction endonuclease BsmBI for five hours at 55°C. The digested product was run on a 0.75% agarose gel containing SYBR green, and gel purified with a Qiagen kit. The CRISPRi primers were annealed at 95°C for two minutes, and then the

temperature was decreased to 25°C at a rate of 0.1°C per second. The digested plasmid and annealed primers were ligated at room temperature overnight and a control reaction lacking primers was also set up. The ligated CRISPRi backbone mixture was used to transform Mach1 *E. coli* cells, and the cells were plated on LB-agar containing 50 µg/ml kanamycin (Kan50). Select colonies were inoculated into LB- Kan50 overnight, mini-prepped, and then sequenced. The sequencing results confirmed the presence of the plasmid, which was used to transform electrocompetent Msm strains WT, D161E and -AA23-25. The Msm cultures were grown on 7H11 plates and transformants were used for subsequent experiments to test knockdown levels achieved. Msm transformants chosen were grown in 25 µg/ml kanamycin for any further use in subsequent experiments.

Gene	Targeting sequence	Forward (-) and Reverse (+) Primers	PAM sequence	PAM strength
panB	1	- 5' GGGAGCGTCGCCGCGGCCCTGCAC 3' + 5' AAACGTGCAGGGCCGCGGCGACGC 3'	+ 5' TTTCCGC 3' - 5' GCGGAAA 3'	110.5
	2	- 5' GGGAGAGTCACCCACCAGGAGCA 3' + 5' AAACTGCTCCTGGTGGGTGACTC 3'	+ 5' ATTCCGG 3' - 5' CCGGAAT 3'	47.3
panC	1	-5' GGGAGCGCGGTCGGGGCGAACGAT 3' +5' AACATCGTTCGCCCCGAVCGCGC 3'	+ 5'CTTCTCG 3' - 5'CGAGAAG 3'	216.7
	2	- 5' GGGAACCCGCGAAATGGCCTGGGCG 3' + 5' AAACCGCCCAGGCCATTTCGCGGGT 3'	+ 5' TTCCTCG 3' - 5' CGACCAA 3'	38.5

Table 2. **Primers and PAM sequences used for CRISPRi design.** Two primers were designed for each *panB* and *panC* construct and PAM sequences were designed to be of varying strengths. PAM strength was previously measured as fold knockdown standardized against a *Renilla* target.

216.7 is the highest recorded knockdown value and 38.5 is the lowest recommended value for CRISPRi (Rock et al., 2017).

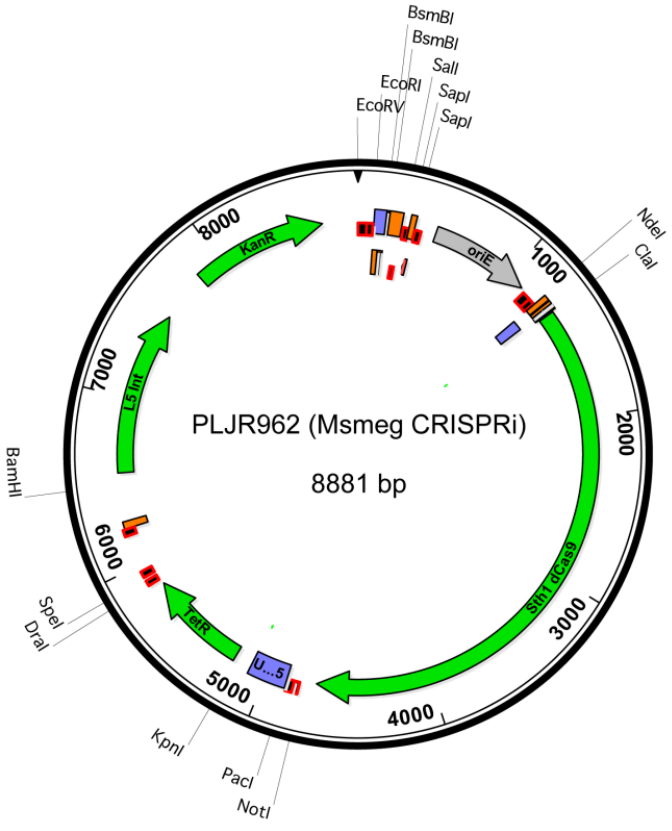

Fig. 3. **Plasmid Vector Backbone PLJR962** (reproduced from Rock, 2017). The Msm plasmid vector PLJR962 was used for CRISPRi cloning to generate *panB* and *panC* knockdown strains. This Tet-Off plasmid encodes an sgRNA that causes ATc-inducible repression of the target gene, as it is under the control of a promoter that activates expression in the absence of ATc. The sgRNA and dCas9 enzyme are induced with ATc to repress expression of *panB* and *panC*. This plasmid also has a kanamycin resistance cassette.

ATc synthetic lethality screening CFU assay: Msm WT and Msm D161E and -AA23-25 *panB* and *panC* knockdowns (both experimental and control strains) were grown in 7H9 supplemented

with 100 ng/mL ATc for one day, then plated on 7H11 containing 100 ng/ml ATc. Plates were incubated for two days at 37°C, and then colonies were counted. A Tet-ON DnaK knockdown strain that has active transcription in the presence of ATc was used to confirm that the ATc stock was not degraded (strain shared from Fay & Glickman, 2014). This experiment was repeated.

An ATc dose response was tested in a 96-well-plate: Msm WT, D161E and -AA23-25 of OD580 of 0.001 and 0.01 Msm were inoculated into a plate serially diluted with 2 to 100 ng/ml ATc and incubated at 37 °C for two days, then at 22°C for one day. The OD of the plates was read at this time.

An ATc disk diffusion assay was conducted, testing concentrations of 0, 0.5 µg, 2.5 µg, and 5 µg ATc. 150 µl of 0.1 OD580 Msm WT, D161E and -AA23-25 *pan*- knockdown strains were plated on 7H11 or 7H11 supplemented with 30 µg/ml pantothenate. Plates were incubated at 37 °C for two days and zones of inhibition (ZOI) for each plate were recorded at that time. Plates were then stored at room temperature for three days, and then 4°C for one day before images were taken of each plate.

Binding Partners of PptT and PptH

Strains used for western blots and IPs: Mtb whole cell lysates (WT, *pptH* knockout (k/o), *pptH* complement (comp), H246N PptH putative LOF point mutant, and Msm whole cell lysates (overexpressing (o/e) mutant pptH H246N, WT, and pptH k/o) and Schnappinger Mtb PptT knockdown (kd) strain).

Limit of detection of PptH and PptT antibodies: His-tagged PptT was purified by John Mosior from Texas A&M University and truncated PptH was purified by Elaine Ballinger of Weill Cornell Graduate School of Medical Sciences. PptT peptide antibody was raised against a

synthetic peptide based on a sequence near the N-terminus of the protein, and an antibody was also raised against the full PptH protein. Both antibodies were from rabbit and generated at New England Peptide. Two-fold dilutions of PptT were used, ranging from 39 ng to 10 µg. The western blot was blocked with the primary antibody overnight in a 1:500 dilution in 3% milk (in Tris-buffered saline-Tween (TBST) buffer), and then an anti-rabbit secondary antibody in a 1:10,000 dilution in 3% milk for one hour. Thermo-Fisher SuperSignal West Femto Maximum Sensitivity Substrate solution was used to develop the blot.

Mtb Lysate Preparation (conducted by Kristin Burns-Huang): Strains were inoculated into 25 ml of 7H9 and OD was monitored over the course of a week. When cultures reached log phase, OD was recorded for each and 20 OD580 units were collected for each strain. Cells were harvested and washed in 1X PBS/Tween80. 400 µl of 50 mM Tris HCl/ 100 mM NaCl/ 10% glycerol/ 2 mM EDTA was added to each sample. Samples were bead-beated for 30 seconds three times, and placed on ice for two minutes in between each beating. 120 µl of supernatant was removed for each sample and 40 µl of 4X sample buffer was added to each. Samples were boiled for ten minutes and then placed on ice for immediate use.

PptT western blot using anti-PptT peptide and PptH western blot using anti-PptH peptide in Mtb whole cell lysates: The western blot was blocked overnight in 3% milk (in TBST buffer), then blocked with the primary antibody overnight in a 1:500 dilution in 3% milk, and then an anti-rabbit secondary antibody in a 1:10,000 dilution in 3% milk for one hour. Thermo-Fisher SuperSignal West Femto Maximum Sensitivity Substrate solution was used to develop the blot.

IP of PptH: Mtb whole cell lysates used with the PptH peptide antibody.

IP of PptT: Mtb whole cell lysates were used with the histidine tag antibody. Lysates were incubated with 400 µg PptT for 1 hour before protein A/G beads were added. The his-antibody was used to IP and blot for PptT.

Protocol for all IPs, adapted from Kristin Burns-Huang: 30 µl of lysate sample was aliquoted out for later use. Pierce Protein A/G Magnetic Beads were washed in PBS and protease inhibitor and 30 µl was added to the remaining 130 µl of lysate solution. The sample was stored at 4°C, rotating, for one hour. Beads were removed and 30 µl of sample was removed for later use. Antibody was added in a 1:100 dilution and the sample was stored at 4°C, rotating, overnight. 25 µl of magnetic beads were pre-washed in PBS, protease inhibitor, 4% glycerol and 0.05% of surfactant Triton X-100. Samples were incubated at 4°C, rotating, for one hour. Beads were removed and 30 µl of sample was removed for later use. The beads were washed with 500 µl of PBS, protease inhibitor, 4% glycerol and 0.05% Triton X-100 three times. 30 µl of sample was removed from the first wash for later use. PBS was used to elute protein from a third of the beads. 100 µL of 0.1 M glycine at pH 2.5 was added to the remaining beads. The beads were rotated for 10 minutes at room temperature. The supernatant was removed and 15 µl of 1 M Tris hydrochloride at pH 8 was added to neutralize the solution. Sample buffer was added and samples were boiled for ten minutes before being run on an SDS page gel.

A semi-dry transfer method was used to transfer protein bands onto a blot. The western blot was blocked overnight in 3% milk in TBST buffer, then blocked with the primary antibody overnight in a 1:500 dilution in 3% milk, and then an anti-rabbit secondary antibody in a 1:10,000 dilution in 3% milk for one hour. Thermo-Fisher SuperSignal West Femto Maximum Sensitivity Substrate solution was used to develop the blot.

Co-IP of PptT and PptH: The previous procedure was followed, with the same samples. The his-antibody was used to IP for PptT and the PptH peptide antibody was used to blot for PptH. The PptH peptide antibody was used to IP for PptH with the His-antibody to blot for PptT.

Statistical analysis and generation of figures: Figures with chemical structures were designed using ChemDraw computer software version 18.0. Graphs were generated using GraphPad Prism Version 7. Comparison of experimental groups was conducted by analysis of variance (ANOVA) using JMP statistical software from SAS (JMP®, Version *14*. SAS Institute Inc., Cary, NC, 1989-2019.)

Results and Discussion

Before testing the Msm strains for chemical stress phenotypes, I first confirmed that the mutant Msm strains were all resistant to 8918. The MIC for 8918 on WT Msm was found to be 0.7 μM, as shown in Fig. S2A. The inhibitor compound displayed significant inhibition of growth of the mutant strains only above 20 μM. In Fig. S2B, moxifloxacin was used as a control because Msm is known to be susceptible to this compound. The MIC for the WT and mutant Msm strains with moxifloxacin was shown to be equivalent, at 0.3 μg/mL.

The control PCR results from each of the mutant strains and the WT in Fig. S3 demonstrate that *pptH* is present in each strain, at its expected size. It was necessary to confirm the presence of *pptH* in the mutant strains before chemical testing, to show that the gene was present but not functional. The size of the gene *rv2795c* was found to be about 960 base pairs. In the PCR amplification gel image in Fig. S3, it measures about 1050 bp because of the addition of a 90 bp primer. Only Msm WT and Msm –AA23-25 are pictured, but the *rv2795c* fragment was detected at the expected size in all four of the strains.

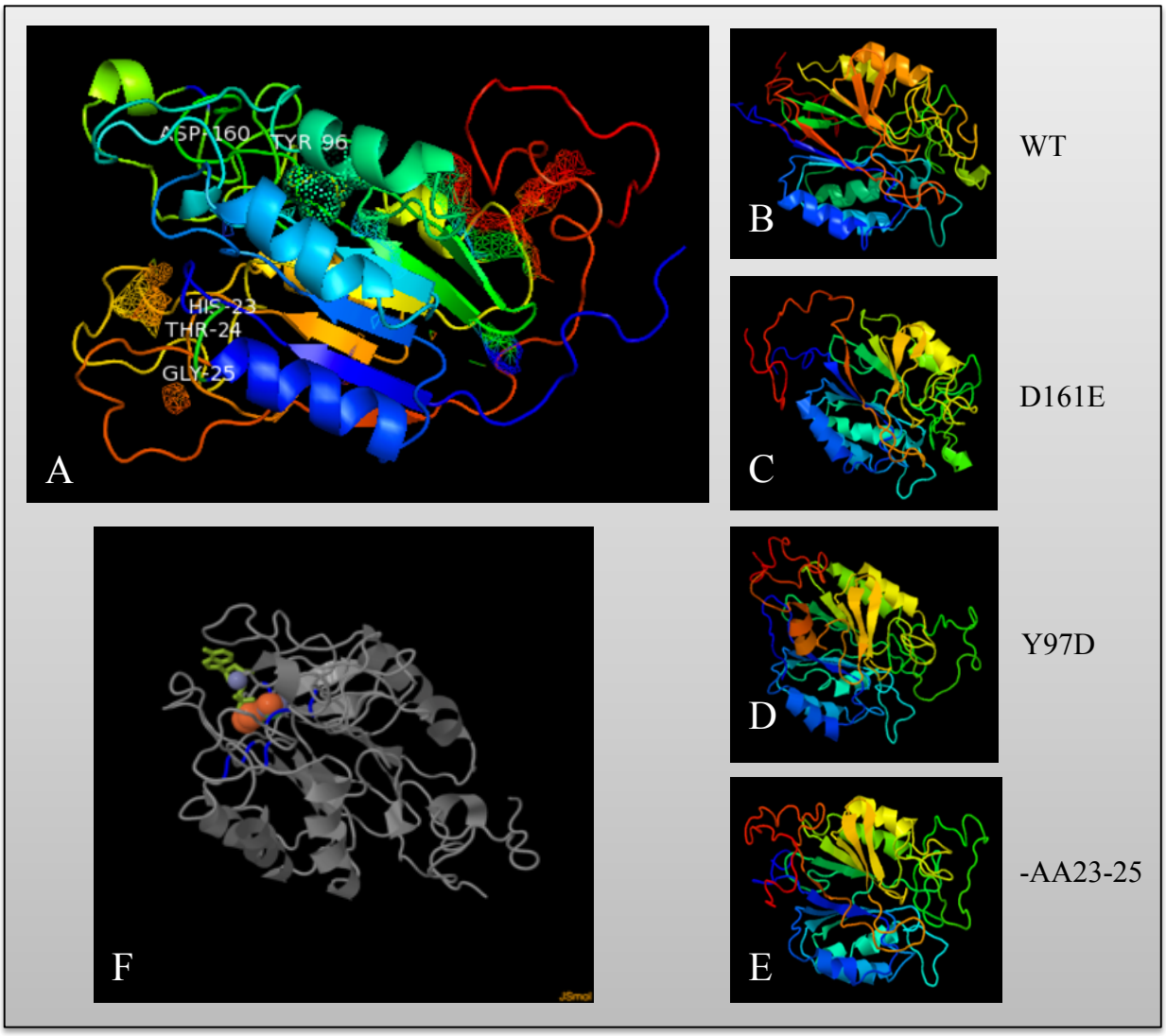

Fig. 4. **Mutant PptH protein structure predictions**. Proteins were modelled using Phyre and PyMOL. **(A)** Sites of the three mutant protein residues are labelled on the WT PptH structure for understanding proximity to the enzyme active site, as all mutated residues are in the vicinity of the active site of the protein. **(B-E)** Individual mutant predicted structures are shown with each specific amino acid mutation labeled below each structure. The rainbow coloring depicts distance along the residue sequence, with the N-terminus colored as blue, progressing through the colors of the rainbow to red, for the C-terminus. The structures have been arranged to be in the same orientation to compare structural differences with as much accuracy as possible. **(F)**

Predicted ligand binding site for PptH is shown by the orange phosphorus atoms. This region denotes the active site of the enzyme. This structure was generated through PyMOL surface cavity detection with a radius of 4 solvent radii.

The mutant protein structure predictions produced from Phyre and PyMOL shown in Fig. 4 display particular variation in the C-terminal folding patterns. It should be noted that the modeling program is limited in its ability to predict fully accurate structures. In Fig. 4B-E, the mutant protein structures are shown to be similar to that of the WT, although slight modifications do exist and are impactful in the active site of the enzyme, as they are deleterious to the function of the enzyme. The D161E mutant C-terminus region appears most different from the others, which is an interesting consideration as the mutation is a conserved change (both aspartic acid and glutamic acid are negatively charged amino acids). The location of mutated residues in Fig. 4A shown to be at the predicted enzyme active site is expected, as these mutations are believed to severely impact the function of the enzyme and this is the most functionally important part of the enzyme, which is shown with its predicted bound ligand in Fig. 4F.

Under the same growth conditions, the mutant strains did not have a growth phenotype different than the WT strain, although this was only tested at 27°C and 37°C. The growth rate curve of the mutant strains presented were found to be the same as the WT strain at 27°C with shaking growth conditions, and a stationary phase value of OD600 of 0.9 was found, as shown in Fig. S4. Similar results to those seen in Fig. S4 were obtained in repeat growth curve experiments at 37°C, although clumping of the cells in the 96 well plates was often experienced at this higher temperature. Although all strains reached a greater OD at this higher temperature, there were no significant differences in growth rate and final OD between WT and PptH putative

LOF mutants. A possible difference in cold growth phenotype between the mutants and WT was not explored, nor was a difference in stationary phase phenotypes, as growth was only studied for 48 hours.

Tests to determine the conditions under which PptH is essential: Chemical stresses

Mtb lives in the host in a state of acidic pH, low oxygen, poor nutrient availability, and abundant reactive oxygen and nitrogen species (Ehrt & Schnappinger, 2009). To simulate this model, I used phosphate-buffered saline (PBS) to create a nutrient starvation in vitro, acidified sodium nitrite as a source of nitric oxide and reactive nitrogen and oxygen intermediates, and lysozyme to replicate native hydrolytic lysosomes that break down peptidoglycan. To target the cell wall specifically, I chose sodium dodecyl sulfate (SDS), an anionic detergent that denatures proteins and disrupts cellular membranes ("Sodium Dodecyl Sulfate"). I also used sodium chloride and water to create osmotic stress (White, He, Penoske, Twining & Zahrt, 2010). An ethidium bromide (EtBr) uptake assay was selected to gauge changes in cell wall integrity, as it is a common assay to measure cell wall permeability. For most chemical stress tests, Msm WT in the presence of a sublethal concentration of 0.3 μM of 8918 (half of the WT minimum inhibitory concentration (MIC) value) was used to indicate that the compound was effective and explore if any combined effects with the stress occurred in the absence of functional PptT.

Chemical	Mutant Phenotype	Decreased survival of the WT
PBS	No	No
Acidified NaNO2	No	Yes
Osmotic	No	No
SDS	Yes	Yes
Lysozyme	No	Yes
EtBr	Yes	Yes

Table 3. **Summary of Msm responses to chemical stress tests.** Select chemicals were used to test for the conditions under which functional PptH is essential.

Msm PptH putative LOF mutants respond to PBS with similar survival phenotypes as WT. There was no significant difference between the survival of WT and PptH putative LOF mutants in the presence of PBS-1% tyloxapol, which was used to simulate a nutrient starvation model. Less survival occurred after 8 days in PBS as opposed to after 48 hours, but this difference was not significant compared to the input survival value, the number of surviving cells after 48 hours, or amongst strains. PBS did not cause a stressed survival phenotype. This result was found again when the test was repeated under the same experimental conditions.

Msm PptH putative LOF mutants respond to acidified sodium nitrite with similar survival phenotypes as WT. No significant difference existed between the survival of WT and putative PptH LOF mutants in the presence of acidified sodium nitrite after 5 days. There was not a significant difference in survival between cells exposed to 3 mM $NaNO_2$ versus 6 mM $NaNO_2$. $NaNO_2$ was shown to hinder survival, by about a log more than cells in the acidified control

media. Only for the WT sample did cells exposed to $NaNO_2$ have greater survival than those in acidified 7H9. About a half log of killing was observed in Msm WT in 3 μM of 8918.

Msm PptH putative LOF mutants respond to osmotic stress with similar survival phenotypes as WT. There was no significant difference in survival between mutant strains and the WT under any of the tested conditions. An average of a half log decrease in survival occurred in the presence of 0.5M NaCl, but there was no significant decrease in survival in the presence of water compared to survival in the control solution of 7H9. For Msm WT in 3 μM of 8918, almost one log of killing occurred. Water did not cause a stressed survival phenotype.

The chemical stresses of PBS, $NaNO_2$, lysozyme, NaCl and water did not induce a significant difference in survival between the mutant and WT strains. Exposure to PBS did not result in decreased cell survival, nor did exposure to water. NaCl was demonstrated to induce a higher degree of killing than water, and both allowed less Msm survival than the control 7H9 solution, although this stressed result was not significant (Table 3). PBS and osmotic stress tests may not have been harsh enough tests to elicit a phenotype from either mutant or WT strains, as opposed to other tests where both strains were affected. $NaNO_2$ was shown to stress cells independently of acidity. The MIC value I found for lysozyme was inconsistent with previous reports of lysozyme MIC assays on Msm, as I found the MIC for all strains to be about 50 μg/mL, which is 40 times lower than the reported value of 2 mg/mL for a WT PM759 Msm strain. The mutant strains and WT responded similarly to treatment with lysozyme. This discrepancy may be due to the use of a different Msm strain. The transposon mutant lysozyme MIC values found in this previous study ranged from 31.25- to 250 μg/mL, which is consistent with the value that I found (Flores et al., 2005).

To demonstrate that phenotypes seen during a chemical stress test are specific to PptH and not due to a mutation at another site in the genome, the chemical stress phenotypes should be confirmed with complemented Msm strains. This could be done by recombination-mediated genetic engineering of the WT allele back into the mutant strains to determine if the stressed phenotype is reversible, or by expressing WT in the mutant background to complement.

A.

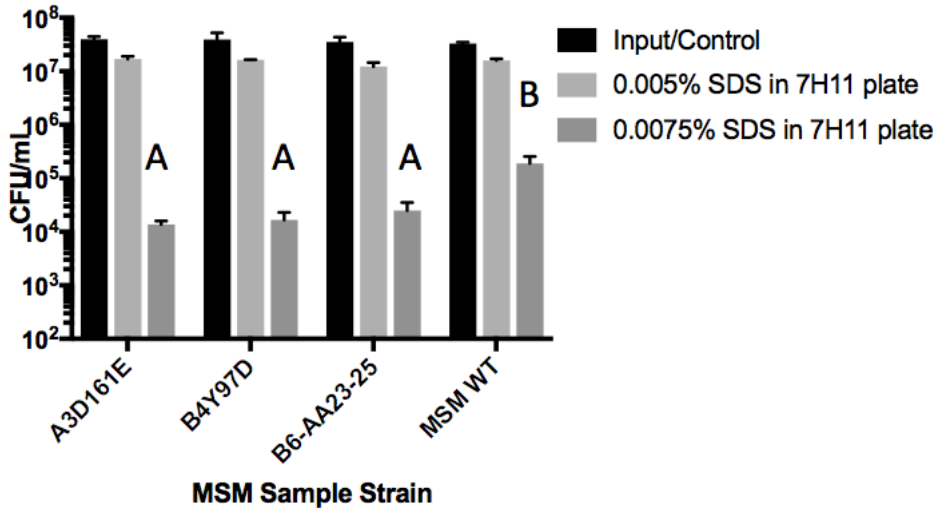

B.

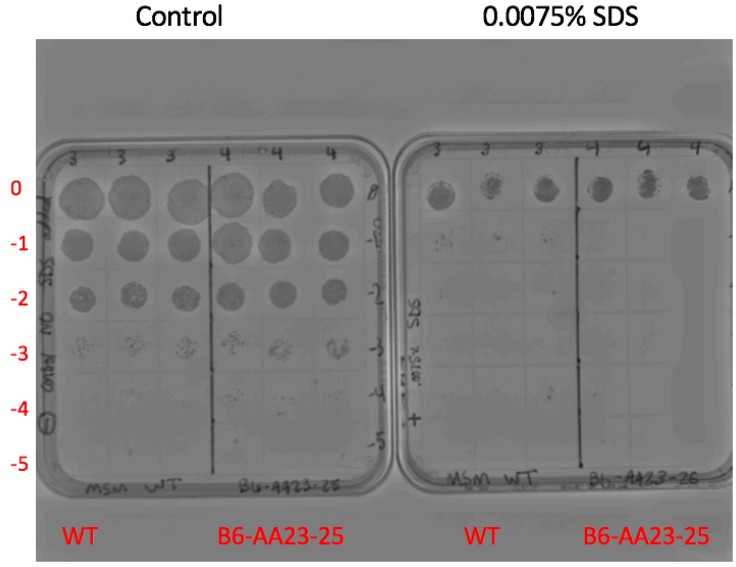

C.

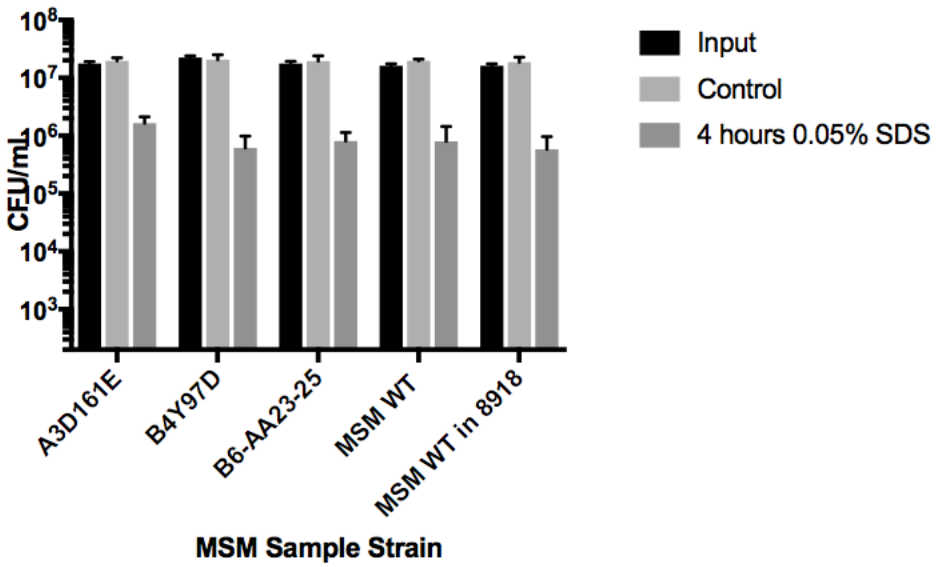

Fig. 5. Response of PptH putative LOF mutants to SDS stress. (A) Mutant cells are more susceptible to SDS stress than WT cells when plated on 7H11 agar containing SDS. Cell survival was quantified for each strain from spot dilutions exposed to different concentrations of SDS. The difference in the survival response to 0.0075% SDS between WT and mutant strains was shown to be statistically significant ($P< 0.0001$) by a comparison of least squares means with a Tukey correction. Samples not denoted by the same letter (A and B) are significantly different. Error bars show standard deviation from the mean (N=3). Further statistical testing is shown in Fig. S5. **(B)** The spot plating of the WT versus strain -AA23-25 for an SDS-treated and non-treated control 7H11 agar plate are shown above. Red numbering indicates ten-fold dilution value. **(C)** Mutants and WT Msm similarly respond to SDS in liquid cultures. Control groups lacked SDS but received the same treatment conditions as the SDS group. Treatment with SDS was shown by a comparison of least squares means with a Tukey correction to have a statistically significant effect on growth ($P<0 .0001$). Differences in survival between strains were not

statistically significant. Error bars show standard deviation from the mean (N=3). Further statistical analysis is shown in Fig. S6.

Discussion of SDS stress test results

When plated on 7H11 agar containing 0.0075% SDS, PptH putative LOF mutants had lower survival rates than the WT. In preliminary testing, D161E was most susceptible to SDS, followed by Y97D, and then -AA23-25. In this test, the WT survived to a degree of one log greater in 0.0075% SDS than -AA23-25. Although there were slight differences in survival rates amongst the mutants in this initial test, these results overall support the results shown in Fig. 5A that the mutant strains had significantly lower survival than the WT. Fig. 5A shows discrepancies in growth between strains at 0.005% and 0.0075% SDS, with all mutant strains surviving one log less than the WT. These results were repeatable. 0.005% SDS in 7H11 does not cause significant stress to Msm survival. In the second plate shown in Fig. 5B, a ten-fold dilution of cells produced several colonies for the WT strain, but no colonies for the mutant strain. Fig. 5C shows a 1.5 log reduction in growth among mutants and the WT compared to the untreated control when exposed to 0.05% SDS for 4 hours, but the mutants did not respond differently to SDS than the WT in liquid cultures.

The investigation of the conditions in which PptH is essential through chemical stress tests yield results that indicate PptH may be involved in cell wall integrity. The phenotypes produced from each of the stress tests were not consistent, but the SDS tests suggest that the lack of functional PptH produces cells with a defective cell wall or an impaired cell wall repair process as measured by lowered cell counts in chemical tests. The decreased cell survival compared to WT Msm observed in the mutants in 0.0075% SDS in 7H11 plates is significant across all mutant strains (Fig. 5A). SDS is a detergent that breaks down lipids and interactions

between proteins; its negative charge linearizes proteins and gives them a uniform anionic charge. It is an established "cell-wall perturbing" agent, and decreased survival in the presence of SDS is attributable to a cell-wall defect (Vandal et al., 2008). Repetition of this experiment with the addition of 0.005% SDS in 7H11 revealed that this concentration is too low to produce a disparate growth phenotype for mutant strains, and provides a minimum concentration to explore a dose response spectrum to SDS stress in Msm.

Interestingly, this same stressed survival phenotype was not observed when SDS was introduced in liquid culture (Fig. 5C). This discrepancy in response to SDS could be due to oxidative effects on cells at air-agar boundaries as experienced on plates as opposed to a liquid culture, where levels of oxygen are lower. Other possible explanations include differences in a molecular space-filling model of atoms due to different states of matter that allow for increased cellular interaction and signaling in a liquid culture, that may reduce susceptibility to stresses.

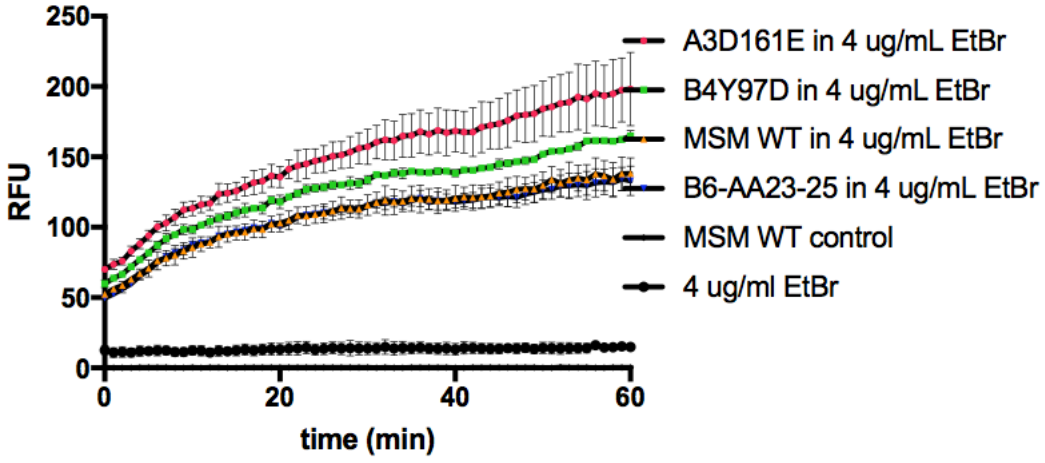

Fig. 6. **EtBr uptake assay revealed that PptH putative LOF mutants emit greater fluorescence than the WT.** The difference in RFU between mutant and WT experimental strains after 60 minutes was not statistically significant. A greater RFU value is indicative of increased

cell wall and membrane permeability. Error bars show standard deviation from the mean (N=3). Further statistical testing is shown in Fig. S7.

In Fig. 6, D161E had the greatest relative fluorescence of 200 RFU (Relative Fluorescence Units) after one hour, followed by Y97D with 160 RFU. Strain -AA23-25 and Msm WT had a similar fluorescence value of 130 RFU after one hour. This result may be indicative of the involvement of PptH in cell wall integrity, through the increased fluorescence of mutant samples. EtBr uptake assays are used to measure cell wall and membrane permeability, as the intercalating agent EtBr fluoresces at a greater level when taken up by and bound to nucleic acids in bacteria (Danilchanka, Mailaender & Niederweis, 2008). D161E had the greatest fluorescence, indicating that it has a more permeable cell membrane than the other mutants and WT. The difference in fluorescence units between the WT sample measured about 75 RFU. These results support my hypothesis that PptH is involved in cell wall integrity, as along with the SDS stress test results, they imply that the absence of functional PptH confers a cell wall defect. This test was only conducted once and the inoculation order of samples in the 96-well plate did mirror the RFU results, which is a possible confounder of results. Repeating the assay with more replicates in a randomized order could correct for this possible error and is necessary to reveal if differences in fluorescence between strains are significant.

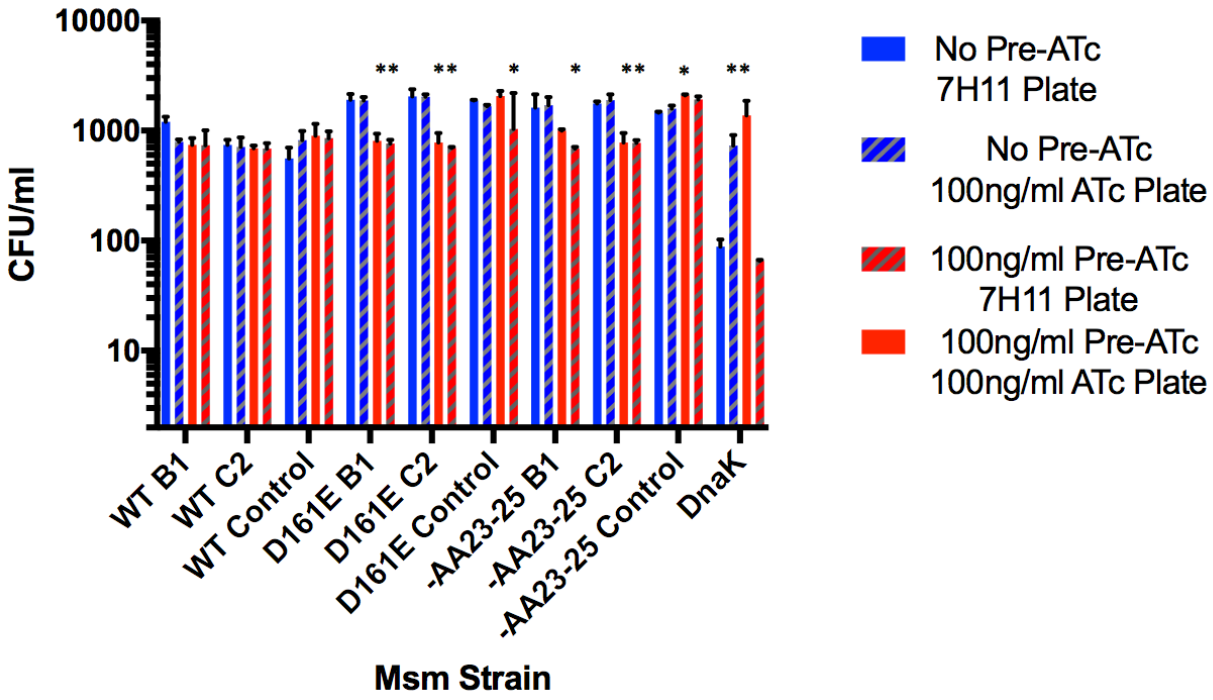

Fig. 7. **CRISPRi strain response to ATc in liquid media.** The blue bars represent strains that were not exposed to ATc before plating. The red bars show strains grown in 100 ng/ml ATc in 7H9 for one day before plating. The striped bars represent samples plated on 7H11 containing ATc. In strain names, "B1" and "C2" refer to the presence of a *panB* or *panC* CRISPRi targeting sequence. A Tet-ON DnaK knockdown strain was included to show the integrity of the ATc stock, and is expected to behave in a manner opposite to the other stains, as the presence of ATc should enhance its growth. Differences in the growth response within the –AA23-25 C2 strain, D161E B1 and C2 strains, and DnaK strain across treatment groups were statistically significant (P=0.0001), as shown through ANOVA F-test slicing. The difference in the growth response of the D161E control strain across treatments (P=0.0016) and of the –AA23-25 B1 strain across treatments (P=0.0005) was also significant. Specific samples denoted by an asterisk indicate

significant differences in growth response within a strain as compared to the control treatment of no ATc for that strain. This analysis was done through a Dunnett's Multiple Comparisons test with the control ($P<0.05$) and highlights the samples that were shown to account for the significant differences seen through the F-test slicing. Error bars show standard deviation from the mean (N=3). Further statistical analysis is shown in Fig. S8.

A. **B.**

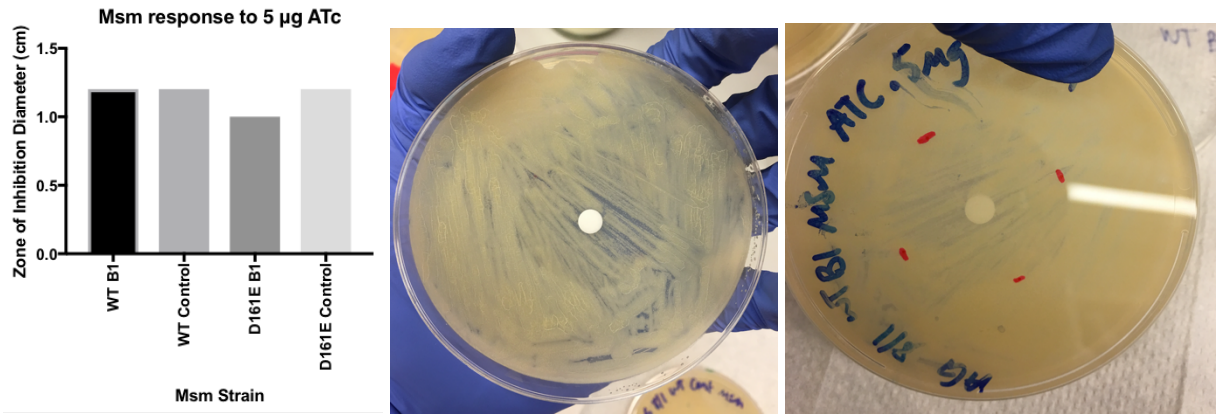

Fig. 8. **ATc Disk diffusion assay with CRISPRi *panB/C* constructs**. **(A)** Disk diffusion assays were conducted on WT and deletion mutants with ATc at concentrations of 0, 0.5, 2.5, or 5 µg ATc and the diameter of the zone of inhibition was recorded for each. Differences in the ZOI diameters between strains were not significant and the inhibition response to 5 µg ATc for select strains is provided. **(B)** A novel "secondary ZOI" was observed in Msm strains containing a *panB* or *panC* knockdown sequence at all concentrations of ATc when plates were grown to stationary phase and stored at cold temperatures.

Discussion of CRISPRi PanB/C constructs and experimental results

Recent studies from collaborators of the Nathan laboratory have found that conditional knockdowns of pantothenate B (*panB*) and pantothenate C (*panC*) in Mtb are bacteriostatic, as CoA levels are depleted, and amino acid and cell wall biosynthesis is impaired (Evans et al., 2016). These researchers generated their knock-down strains by replacing native promoters with a Tet-regulated promoter by single crossover homologous recombination. They hypothesized that genes expressed at low basal levels in Mtb may be more efficiently silenced by newer gene silencing tools such as Clustered Regularly Interspaced Short Palindromic Repeats interference (CRISPRi). Using PptH putative LOF mutants, I tested for synthetic lethality with ATc-repressible Tet-Off *panB* and *panC* knockdown strains generated by CRISPRi, hypothesizing that PanB and PanC are non-essential if PptH is present and functional and that they are essential if PptH is not present and/or not functional. Growth discrepancies between WT and knockout strains would infer if PptH were essential in the absence of essential enzymes needed for Ppt synthesis (Evans et al., 2016).

Mutant PptH LOF CRISPRi *panB* and *panC* knockdowns were exposed to ATc to induce gene knockdown, and were expected to grow less than WT strains if gene knockdown and synthetic lethality were occurring. Exposure to ATc prior to plating is necessary to knockdown PanB and PanC protein transcript levels to a level low enough to confer a growth defect. Msm D161E and -AA23-25 CRISPRi *panB* and *panC* knockdowns pre-treated with 100 ng/ml ATc in liquid media for one day exhibited half a log less CFU/ml than strains without a knockdown sequence or strains not pre-treated with ATc, as shown in Fig. 7. The presence or absence of ATc in the agar plate did not affect growth. DnaK experienced killing when deprived of ATc, which was expected with a Tet-On strain. Both WT strains possessing a *panB/C* targeting sequence or

control CRISPRi sequence showed no defect in the presence or absence of ATc, nor did mutant strains with the control CRISPRi sequences. Mutant strains with a *panB/C* targeting sequence exhibited significantly less growth when pre-treated with ATc. This experiment was conducted in triplicate, but when repeated, these findings varied slightly each time and were largely not reproducible. Fig. 7 is included to show the growth patterns of the CRISPRi knockdown strains in the presence of the specific ATc conditions shown, as determining if gene knockdown is occurring is a necessary precursor to determining if PptH is functioning in a CoA salvage pathway.

Fig. 8A reveals that Msm strains do not respond differently to ATc through a disk diffusion assay. No true zone of inhibition (ZOI) formed from DMSO or 0.5μg ATc and similar ZOIs formed from 2.5 μg and 5 μg ATc. A small false ZOI formed around all disks containing ATc in response to the toxicity of the compound. The "secondary ZOI" observed in select samples in Fig. 8B was of the same diameter for samples in which it was present.

Results from the CRISPRi cloning experiments do not reveal repeatable *panB/C* knockdown growth inhibition and suggest that neither PanB nor PanC levels were effectively lowered in the Msm cells. This is evidenced by the inability to replicate results shown in Fig. 7 (which suggests that slight knockdown effects are observed in strains with a *panB/C* targeting sequence that had been pre-treated with ATc) through a repeat of CFU assays. This test indicated that mutant strains with a *panB/C* targeting sequence experienced greater growth knockdown effects than mutant control strains lacking the sequence. This difference based on the presence of a *panB/C* targeting sequence was not observed for WT strains. WT strains were expected to have a growth value similar to the mutant control strains, because they have a functional PptH and should not be experiencing synthetic lethality in the absence of PanB/C. For conclusions to be

drawn from the findings shown in Fig. 7, these results would have to be replicated at least two more times, and WT growth should be greater than mutant growth to indicate synthetic lethality. Results indicating differences in growth between mutant and WT knockdowns were not obtained by liquid growth assays to achieve dose responses in 96 well plates, or disk diffusion assays. No dose response to ATc was achieved when conducted in 96-well plates with a starting Msm OD580 of 0.01 or 0.001. Disk diffusion assays with ATc yielded similar zones of inhibition of about 1 cm for all strains tested, as shown in Fig. 8A. There was no consistent growth response associated with ATc concentration for any strain in this test.

Because evidence is not conclusive that *panB* and *panC* were successfully targeted and knocked down, no conclusions can be drawn from these experiments that a CoA salvage pathway does or does not exist. The DnaK Tet-On strain shown in Fig. 7 confirmed that the ATc stock was not degraded. The plasmid vector containing the knockdown sequence should have been retained in transformed Msm cells, as they were grown in the presence of kanamycin due to the kanamycin resistance cassette present in the plasmid. PanB/C levels may not have been knocked down because the PAM sequence was not strong enough or a sequence in the promoter should have been targeted instead of the region that I chose in the open reading frame. It has been previously reported that "each possible permissive PAM position variant may not be functional with all other variants," and testing of each of the 24 variants can determine which works best (Rock et al., 2018, p. 5). Due to experimental material and time constraints, I tested four PAM sequences, but chose them to vary in their reported strengths, ensuring that one had maximum tested fold repression (Table 2). Rock reports a knockdown range of 2.7–216.7 fold (Rock, 2017). In a future repeat of this CRISPRi experiment, it may be necessary to test all 24 variants to produce a successful knockdown strain.

To circumvent possible limitations to CRISPRi that are not fully explored, *pan B/C* could be knocked down in the future by single crossover homologous recombination. This method was used by Evans et al. in 2016 when exploring the efficacy of CoaBC as a bactericidal target. Other possibilities include that *pan B/C* is knocked down but does not confer a growth deficient phenotype. If this were the case, I could determine if knockdown is occurring by qRT-PCR, and if there is upregulation of *panB*, or *panC* in the mutants. If an antibody to Pan B/C were generated, a western blot of PptH in *panB* and *panC* knockdown strains in WT and the PptH putative LOF mutants could be performed. The next most logical step for this experiment is to conduct qRT-PCR to determine if gene knockdown is occurring. Possible flaws in my experimental design may have been a lack of optimization of the duration of the ATc depletion period. Strains were depleted for up to 3 days with ATc, but this may not have been a long enough time course. I selected this duration from normalizing it off of the standard ATc depletion time used in Mtb, and it was expected to be a long enough duration for Msm, based on the growth rate of Msm. Because the ATc growth inhibition experiments may have been conducted with strains in which PanB and PanC levels were not knocked down, synthetic lethality could not be tested for and no conclusions about the role of PptH in a synthetic lethality pathway can be made from these experiments.

Fig. 8B depicts the formation of a "secondary ZOI" in plates that had been exposed to ATc, which was observed in strains possessing a knockdown sequence. This novel effect was noted after the cells had reached stationary phase, and the plates were stored at 4°C. This secondary zone had a lawn of cells that was thinner than the lawn on the rest of the plate, and the air-lawn surface was shiny and glossy in appearance. The zone was not seen in the control samples, plates lacking ATc, or plates that had been supplemented with 30 μg/ml pantothenate.

There is no mention of secondary ZOIs in previous literature, but it is possible that a phenotype emerged in the knockdown strains that was temperature sensitive or only appears during stationary phase. This hypothesis is a point of further exploration.

Exploring the regulation of PptH and PptT in Mycobacteria

A.

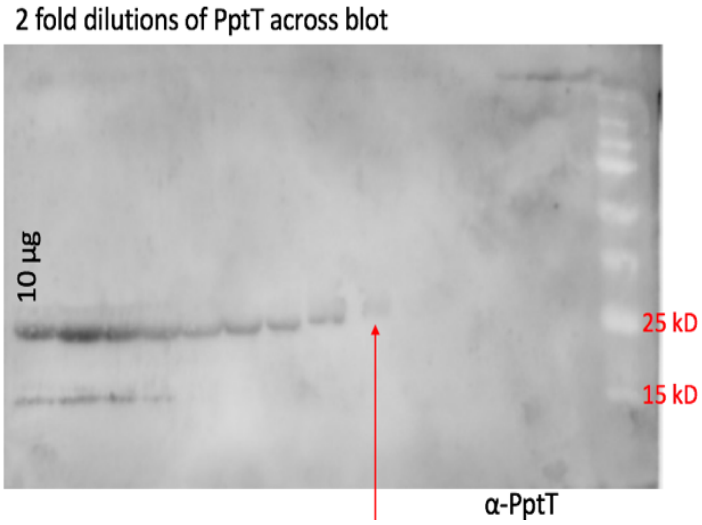

B.

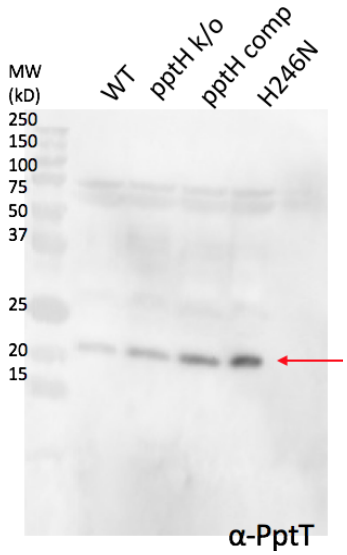

C.

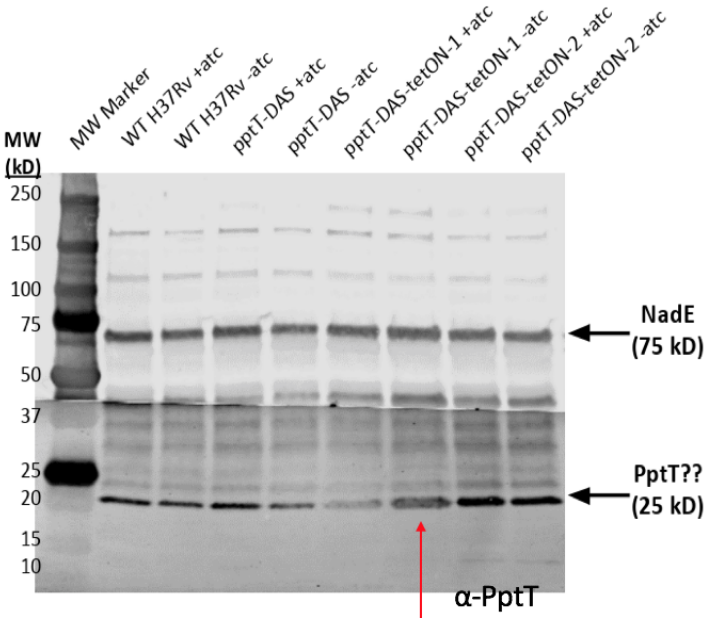

D.

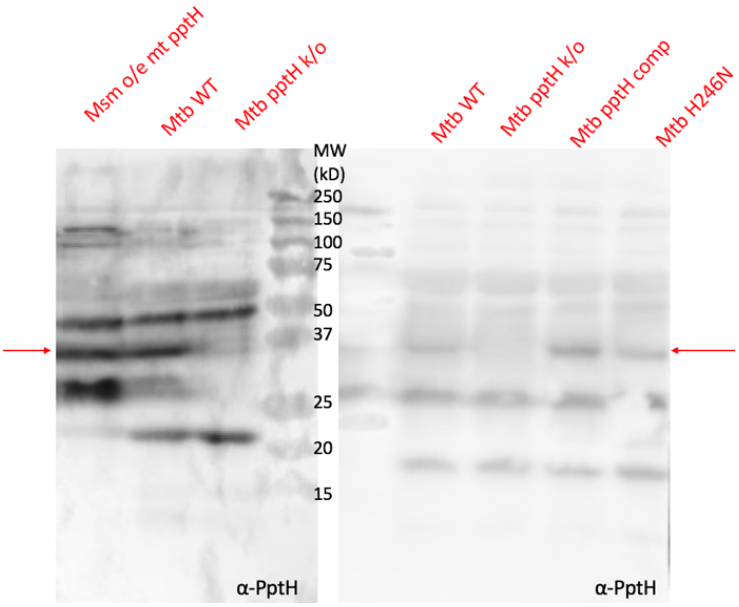

Fig. 9. PptH and PptT peptide antibody recognition. (A) Limit of Detection (LOD) of PptT peptide antibody**.** The western blot SDS-PAGE gel shows purified PptT diluted two-fold, decreasing in concentration from left to right. The PptT peptide antibody LOD on purified PptT from John Mosior of Texas A&M University was found to be 39 ng. The expected size of PptT is 24.7 kD, as observed in the blot. The LOD of the PptH full protein antibody was not readable due to degradation of the PptH protein purified by Elaine Ballinger. **(B)** This western blot of Mtb whole cell lysates using the PptT peptide antibody displays an intense band at 21kD, which is nearly 4 kD lower than expected for PptT. **(C)** PptT peptide antibody does not recognize PptT in Mtb whole cell lysates. This blot of Mtb whole cell lysate samples was produced by Curtis Engelhart of the Dirk Schnappinger Lab of Weill Cornell Medicine. The arrow points to a Tet-ON PptT knockdown strain in the absence of ATc. **(D)** PptH peptide antibody recognizes PptH in Mtb and Msm whole cell lysates. The results of the western blot demonstrate that the PptH peptide antibody is not pure, but recognizes PptH. Samples shown above are Msm whole cell

lysates (left), followed by Mtb whole cell lysates (right). The red arrow denotes the PptH band at 37 kD, which is the expected size. Contaminating band identities were not determined.

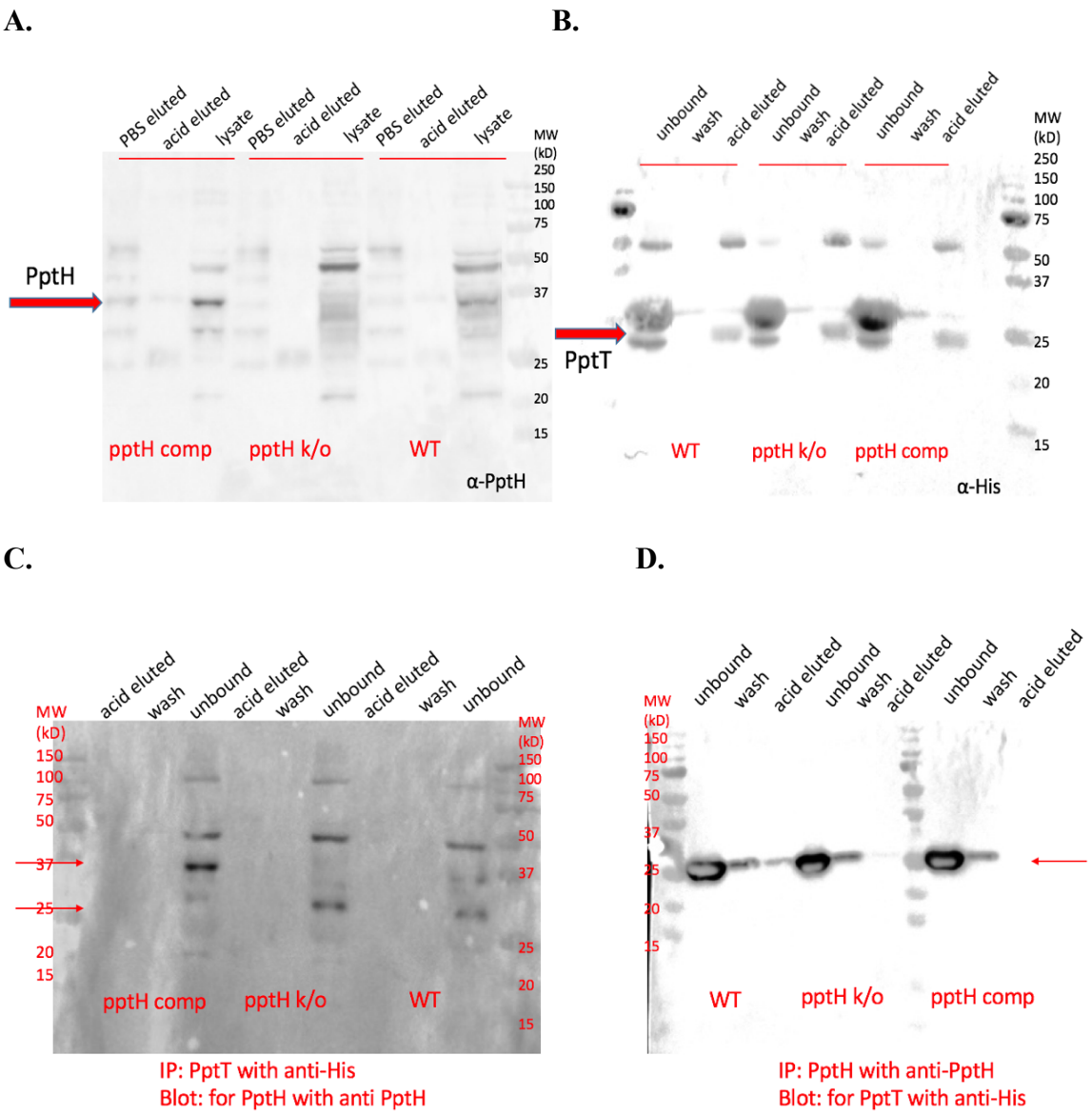

Fig. 10. **PptT and PptH IP in Mtb whole cell lysates and are not shown to interact through co-IP. (A)** The PptH peptide antibody is successful in detecting PptH when used for IPs, as PptH is eluted from Mtb whole cell lysates via acid in WT and *pptH* complemented samples, and not present in *pptH* knockout samples. **(B)** PptT is pulled down when added exogenously to lysate

samples and detected with a his-antibody. **(C)** PptH is not eluted in any sample, and is only present in the unbound original lysate sample. **(D)** This blot reveals PptT eluted in the WT and *pptH* knockout samples, but not the complemented sample, although it is present in the unbound original lysate fraction for all samples tested. The red arrows denote the expected size for PptH and PptT, at 37kd and 25 kd, respectively.

PptT and PptH are Not Found to Interact Through Co-IPs

PptT and PptH were hypothesized to potentially physically interact because they act in the same pathway and are encoded next to each other in the same operon in multiple mycobacterial species. While these conditions do not mean that they necessarily interact with each other, this is a possibility. It is also possible that one of the proteins is modified post-translationally so that it is inactivated and they do not oppose each other's functions.

The PptT peptide antibody failed to recognize PptT in Mtb whole cell lysates, as confirmed through the use of the Schnappinger laboratory PptT knockdown strain (Fig. 9C). The arrow showing the band at 20-21kD from the Tet-ON PptT knockdown strain in the absence of ATc should be fainter than it appears if the antibody is truly recognizing PptT, especially in comparison to the PptT knockdown strain in the presence of ATc. Possible reasons for why PptT is not recognizable include that the antibody is degraded, or modified at the epitope. The most likely explanation is that PptT is not present in great enough quantities natively in the cell to be recognized by this antibody, as it does have a LOD of 39 ng (Fig. 9A).

The experiments involving protein blotting of PptT and PptH were restricted by available antibodies. For the PptH peptide antibody, the most antigenic region of the full protein that the antibody had been created from was not present in the truncated purified protein. This antibody

was also not clean, as shown in westerns detecting PptH seen in Fig. 9D. Attempts were made to purify the antibody using a carboxy-link column. The C-terminus of the peptide was modified to an amide. However, two glutamic acid residues exist in the peptide sequence that could potentially link to the carboxyl resin and enable purification of the antibody. An amino-link column could not be used due to the lack of a free primary amine in the peptide sequence. The peptide sequence also lacks any lysines and has an acylated N-terminus. Affinity purification of the antibody was not successful, likely because not enough peptide was bound to the column. One mg of peptide was available and this was used, but was also the lowest recommended peptide quantity to bind to the column.

Because the antibody designed to the PptH peptide was not clean but recognizes PptH, it was used for the IP of PptH in Mtb whole cell lysates. It was found to effectively detect and allow IP of PptH, as confirmed by the *pptH* knockout sample (Fig. 10A). Purified PptT with a poly-histidine tag was added exogenously to lysates because a his-antibody was available to detect this protein. This experiment was conducted presuming that the exogenous PptT would interact with PptH in the same manner as native interactions may occur in the cell. Under these conditions, PptT was successfully immunoprecipitated, as it was present at its expected size in the acid elutions of all three samples. Before conducting co-IPs of PptH and PptT, it was necessary to confirm that each of these proteins successfully IP individually.

Co-IPs of PptH and PptT did not indicate that the two proteins interact under the conditions tested. In Fig. 10C, PptH was not eluted by acid in any sample. Although Fig. 10D reveals PptT in the acid eluted WT sample, this PptT band would be present in the *pptH* complemented sample and absent from the *pptH* knockout sample if there was an interaction. Because PptT is faintly present in the knockout sample and absent from the complemented

sample, this proposed interaction between the two proteins is false. All experiments with the purified PptT were conducted under the assumption that the protein was functional. If the protein were not functional or degraded, it would likely not bind to PptH. It is possible that the two proteins do interact natively but this interaction was not revealed through the artificial method of exogenously adding PptT. Electrospray ionization mass-spectrometry data could be used to confirm that PptT and PptH are not binding partners, and find other binding partners and possible modifications of the proteins.

Mass spectrometry was not conducted on my samples because the Weill Cornell Medicine Proteomics Core did not believe that major differences would be apparent between my co-IP samples. This was because I was not able to identify banding differences between my samples of WT, *pptH* complement, or *pptH* knockout by silver staining or coomassie staining ("Protocol for Silver Staining"). To obtain new samples for mass spectrometry, Kristin Burns-Huang repeated the co-IP experiments with lysates from a larger volume of cells. She used 50 mL Mtb, which is the maximum volume of culture normally used for this class of experiments. She attached the PptH antibody in serum form to the beads so it would be less likely to elute. This was repeated, and PptH was not eluted either time. Some cross-reactive bands appeared when the blot was heated to elute, but this was not indicative of the presence of PptH. It is possible that the PptH antibody was not efficiently cross-linked to the beads, or that PptH is not consistently amenable to IP under these conditions.

If PptH and PptT do interact, it is also possible that the interactions between them are more transient. If this were true, a small chemical cross-linker is often used to fix weaker interactions. However, the structures of PptT and PptH lack the 'covalent handles' necessary for this linkage. For this type of experiment, crosslinks normally form if the proteins are within a

few angstroms of each other, which implies that they may already be interacting. Pull-down assays could also be used to detail any interactions, as well as a bacterial two-hybrid system. For future assays, a purified PptH protein and peptide sample, as well as a PptT knockdown strain would lead to more clarity in results, and more flexibility in the design of experiments. In future tests, I would like to use the optimized western to see if protein expression varies in different growth stages or stress conditions, and co-IP under these conditions to see if they affect the interactions between PptT and PptH. I am also interested in exploring the other possible binding partners, modifications, and substrates of PptT and PptH in Msm and Mtb.

Conclusion

Overall, these experiments have established groundwork for future experiments to determine the role of PptH in the mycobacterial cell. My chemical stress testing results indicate that functional PptH may be required for complete cell wall integrity in Mycobacteria. Experiments with Coenzyme A metabolism leave many questions open and raise interesting considerations for future studies with bacterial CoA synthesis. Through co-IPs, PptH is not shown to interact with PptT, and I have proposed methods to confirm this in future experiments.

These tests have provided insight into mycobacterial biology as well as a greater understanding of possible functions of PptH that may support its future efficacy as an Mtb drug target. This work further elucidates the characteristics of an enzyme of which the LOF is a novel record of antimicrobial resistance (Ballinger et al., 2019). The Nathan laboratory is continuing to explore substrates of PptH, as well as its role in CoA salvage in Mtb, and desiccation. They have devoted more resources to studying PptH as interest in this enzyme has grown. This project

is a novel area of exploration in mycobacterial metabolism and virulence and is anticipated to provide a greater understanding of mycobacterial biology.

Acknowledgements

I thank Dr. Kristin Burns-Huang for all of her invaluable guidance and mentorship. Her patience and daily positive feedback helped me develop confidence in my work and strive towards independence. I am also grateful for the insight provided to me by Dr. Carl Nathan and the time that he took to help me grow as a scientist. Dr. Elaine Ballinger completed the initial efforts of this research, and I am grateful for the opportunity to extend off of her work. I thank Dr. Ben Gold for his valuable technical input and the entire Nathan lab for being so supportive of my research endeavors. A special thanks to the Schnappinger and Ehrt labs for allowing me to use their equipment. I additionally acknowledge Dr. David Russell for his help in providing feedback on this document and serving as my advisor in Ithaca. I would also like to thank the Cornell Statistical Consulting Unit for their assistance with the analysis of my results.

The generous funding of Cornell University Biological Sciences alumnus Dr. Eskenazi enabled me to pursue the first half of this research project through the Cornell University Biology Summer Internship Program, and the Cornell University DYO Internship program supported my work for the second half.

This project was funded by NIH grant number 1R21AI138939-01.

References

Ballinger, E. (2018). *IDENTIFICATION OF A PHOSPHOPANTETHEINYL TRANSFERASE INHIBITOR THAT KILLS MYCOBACTERIUM TUBERCULOSIS AND A NOVEL MECHANISM OF RESISTANCE INVOLVING AN ENZYME OF PREVIOUSLY UNKNOWN FUNCTION: PHOSPHOPANTETHEINYL HYDROLASE* (Published doctorate thesis). Weill Cornell Graduate School of Medical Sciences.

Ballinger, E., Mosior, J., Hartman, T., Burns-Huang, K., Gold, B., Morris, R., . . . Nathan, C. (2019). Opposing reactions in coenzyme A metabolism sensitize Mycobacterium tuberculosis to enzyme inhibition. *Science,363*(6426), 1-8. doi:10.1126/science.aau8959

Barry, C. E., Boshoff, H. I., Dartois, V., Dick, T., Ehrt, S., Flynn, J., . . . Young, D. (2009). The spectrum of latent tuberculosis: Rethinking the biology and intervention strategies. *Nature Reviews Microbiology, 7*(12), 845-855. doi:10.1038/nrmicro2236

Danilchanka, O., Mailaender, C., & Niederweis, M. (2008). Identification of a Novel Multidrug Efflux Pump of Mycobacterium tuberculosis. *Antimicrobial Agents and Chemotherapy, 52*(7), 2503-2511. doi:10.1128/aac.00298-08

Darwin, K. H., & Nathan, C. F. (2005). Role for Nucleotide Excision Repair in Virulence of Mycobacterium tuberculosis. *Infection and Immunity, 73*(8), 4581-4587. doi:10.1128/iai.73.8.4581-4587.2005

Daugherty, A., Powers, K. M., Standley, M. S., Kim, C. S., & Purdy, G. E. (2011). Mycobacterium smegmatis RoxY is a repressor of oxyS and contributes to resistance to oxidative stress and bactericidal ubiquitin-derived peptides. *Journal of bacteriology*, *193*(24), 6824-33.

Ehrt, S., & Schnappinger, D. (2009). Mycobacterial survival strategies in the phagosome: defense against host stresses. *Cellular microbiology*, *11*(8), 1170-8.

Evans, J. C., Trujillo, C., Wang, Z., Eoh, H., Ehrt, S., Schnappinger, D., . . . Mizrahi, V. (2016). Validation of CoaBC as a Bactericidal Target in the Coenzyme A Pathway of Mycobacterium tuberculosis. *ACS Infectious Diseases, 2*(12), 958-968. doi:10.1021/acsinfecdis.6b00150

Fay, A., & Glickman, M. S. (2014). An Essential Nonredundant Role for Mycobacterial DnaK in Native Protein Folding. PLoS Genetics, 10(7). doi:10.1371/journal.pgen.1004516

Flores, A. R., Parsons, L. M., & Pavelka, M. S. (2005). Characterization of novel Mycobacterium tuberculosis and Mycobacterium smegmatis mutants hypersusceptible to beta-lactam antibiotics. *Journal of bacteriology*, *187*(6), 1892-900.

Gebhard, S., Humpel, A., Mclellan, A. D., & Cook, G. M. (2008). The alternative sigma factor SigF of Mycobacterium smegmatis is required for survival of heat shock, acidic pH and oxidative stress. *Microbiology, 154*(9), 2786-2795. doi:10.1099/mic.0.2008/018044-0

Houben, R. M., & Dodd, P. J. (2016). The Global Burden of Latent Tuberculosis Infection: A Re-estimation Using Mathematical Modelling. *PLOS Medicine, 13*(10). doi:10.1371/journal.pmed.1002152

Leblanc, C., Prudhomme, T., Tabouret, G., Ray, A., Burbaud, S., Cabantous, S., . . . Chalut, C. (2012). 4′-Phosphopantetheinyl Transferase PptT, a New Drug Target Required for Mycobacterium tuberculosis Growth and Persistence In Vivo. *PLoS Pathogens, 8*(12). doi:10.1371/journal.ppat.1003097

Manganelli, R., Voskuil, M. I., Schoolnik, G. K., & Smith, I. (2001). The Mycobacterium tuberculosis ECF sigma factor σE: Role in global gene expression and survival in macrophages†. *Molecular Microbiology, 41*(2), 423-437. doi:10.1046/j.1365-2958.2001.02525.x

Middlebrook OADC Growth Supplement M0678. (n.d.). Retrieved from https://www.sigmaaldrich.com/catalog/product/sial/m0678?lang=en®ion=US

Mycobrowser. (2018, June 5). Retrieved from https://mycobrowser.epfl.ch/

Nathan, C. (2018). *MYCOBACTERIAL PHOSPHOPANTETHEINE HYDROLASE: POTENTIAL FOR SALVAGE OF COENZYME A*. Unpublished manuscript, NIH, Weill Medical College of Cornell University, New York.

Rock, J. (2017). CRISPRi gene silencing in mycobacteria. *V. 4*.

Rock, J. M., Hopkins, F. F., Chavez, A., Diallo, M., Chase, M. R., Gerrick, E. R., Pritchard, J. R., Church, G. M., Rubin, E. J., Sassetti, C. M., Schnappinger, D., … Fortune, S. M. (2017). Programmable transcriptional repression in mycobacteria using an orthogonal CRISPR interference platform. *Nature microbiology*, *2*, 16274. doi:10.1038/nmicrobiol.2016.274

Rockefeller University PROTEOMICS RESOURCE CENTER Protocol for Silver Staining. (n.d.). Retrieved from http://proteomics.rockefeller.edu/ms_silverStaining

Sodium Dodecyl Sulfate, Molecular Biology Grade (SDS). (n.d.). Retrieved from https://www.promega.com/products/biochemicals-and-labware/biochemical-buffers-and-reagents/sodium-dodecyl-sulfate_-molecular-biology-grade-_sds_/?catNum=H5113

Tuberculosis (TB). (2018, October 22). Retrieved from https://www.cdc.gov/tb/publications/factsheets/statistics/tbtrends.htm

Tuberculosis (TB): World Health Organization: Africa. (2017). Retrieved from http://www.afro.who.int/health-topics/tuberculosis-tb

Vandal, O. H., Roberts, J. A., Odaira, T., Schnappinger, D., Nathan, C. F., & Ehrt, S. (2008). Acid-Susceptible Mutants of Mycobacterium tuberculosis Share Hypersusceptibility to Cell Wall and Oxidative Stress and to the Host Environment. *Journal of Bacteriology, 191*(2), 625-631. doi:10.1128/jb.00932-08

White, M. J., He, H., Penoske, R. M., Twining, S. S., & Zahrt, T. C. (2010). PepD Participates in the Mycobacterial Stress Response Mediated through MprAB and SigE. *Journal of Bacteriology, 192*(6), 1498-1510. doi:10.1128/jb.01167-09

World Health Organization. (2010). *Treatment of tuberculosis: Guidelines* (4th ed.). Geneva.

Supplementary Figures

A.

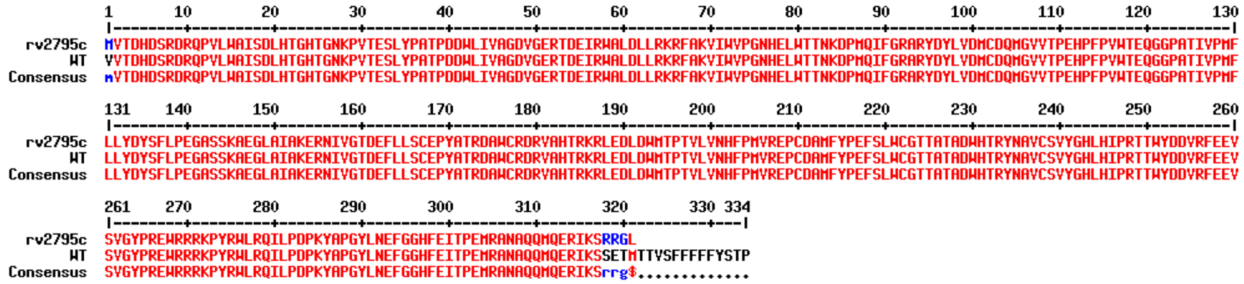

B.

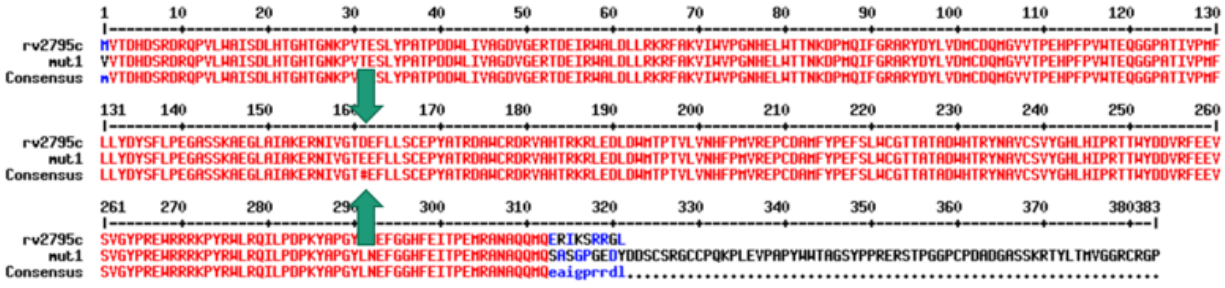

C.

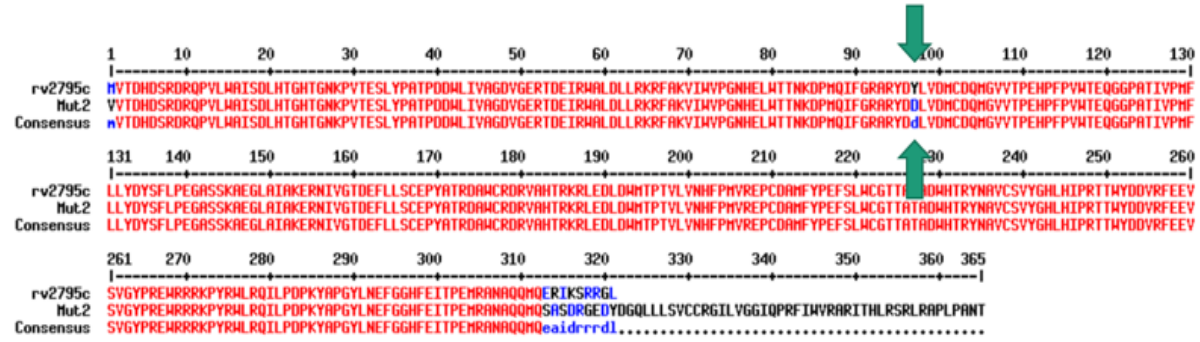

D.

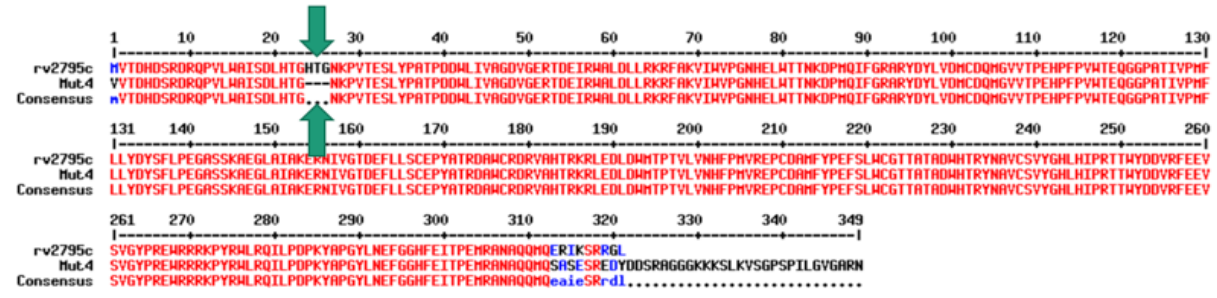

Fig. S1. **Msm WT and PptH LOF mutant protein sequences derived from Multalin.** The green arrows denote sites of mutation. These sequencing results confirmed the specific mutations present in the PptH putative LOF mutants. **(A)** Msm WT reference sequence. **(B)** Msm D161E mutant caused by a substitution of adenine for cytosine at 510bp. **(C)** Msm Y97D mutant caused by a substitution of guanine for thymine at 314 bp. **(D)** Msm -AA23-25 caused the deletion of bps 87-96, resulting in the loss of histidine, threonine, and glycine residues.

A. **B.**

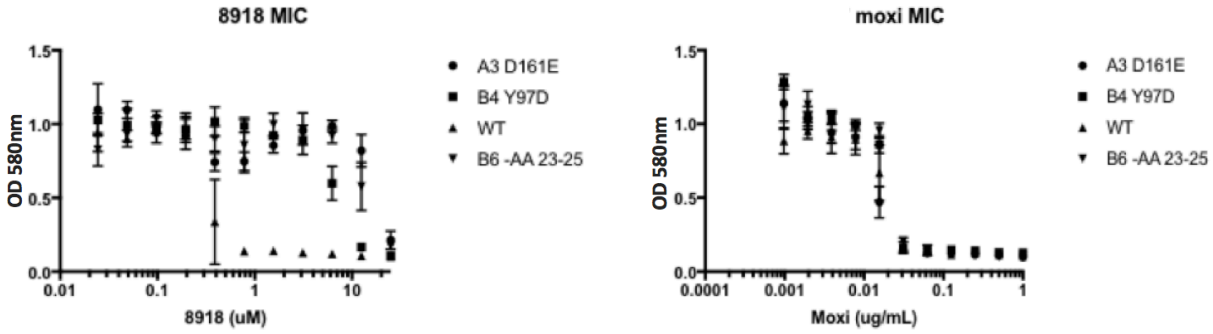

Fig. S2. **MIC of Msm PptH LOF mutants to the PptT inhibitor compound 8918. (A)**The MIC assay for 8918 is shown on the left and the MIC for 8918 on WT Msm was found to be 0.7 µM. The inhibitor compound displayed inhibited growth of the mutant strains only above 20 µM. **(B)** The MIC of moxifloxacin was tested for as a control, shown on the right. The MIC for the WT and mutant Msm strains with moxifloxacin was equivalent, at 0.3 µg/mL. Error bars show standard deviation from the mean (N=3).

A. Msm WT **B**. Msm -AA23-25

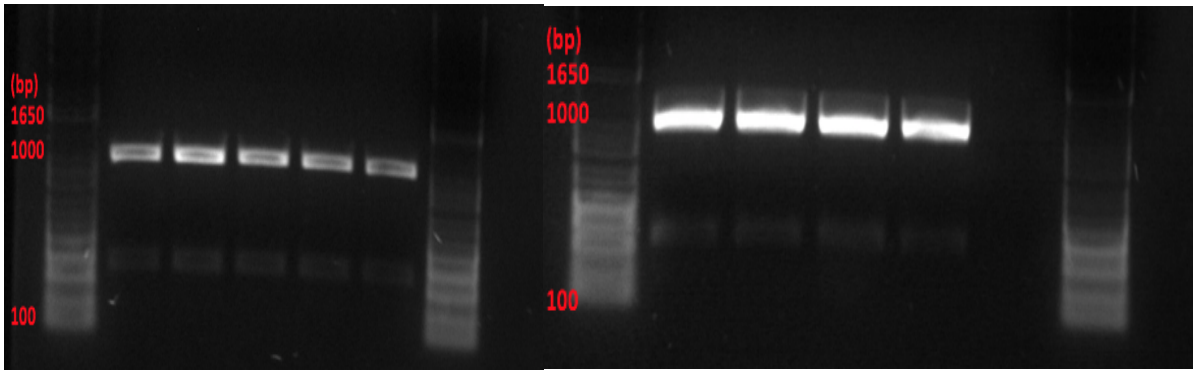

Fig. S3. **PCR amplification of *rv2795c* in WT and deletion mutant samples. (A)** Identical WT genomic DNA samples were loaded into each of five wells shown in the agarose gel. **(B)** Identical Msm –AA23-25 mutant genomic DNA was loaded into each of four wells shown. A band at 1000 bp is seen for each sample loaded in the two gels.

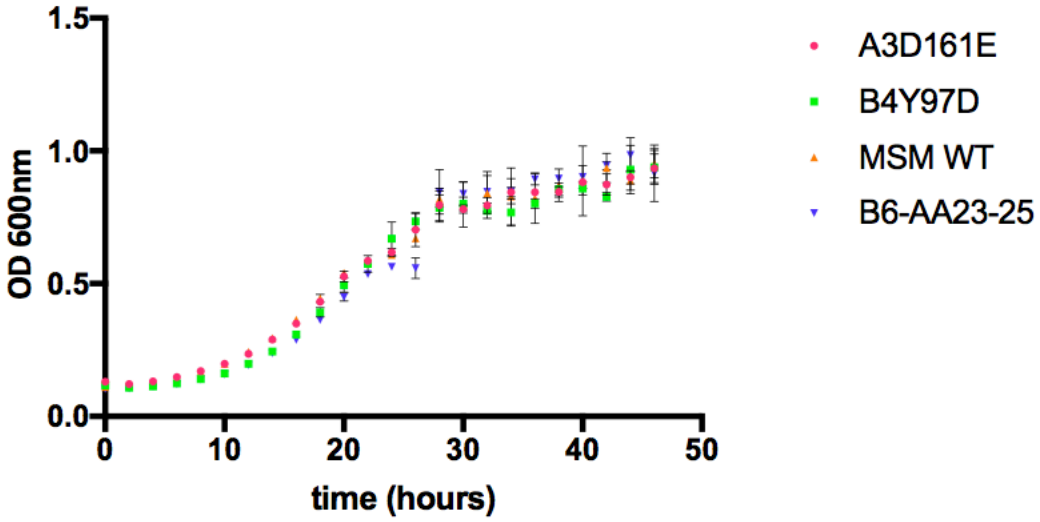

Fig. S4. **Mutant growth curves match that of the WT.** The growth rate curve of the mutant strains presented were found to be the same as the WT strain at 27°C with shaking growth conditions. All values shown were collected in triplicate and optical density was measured every

hour, although readings for only every two hours are shown. Error bars show standard deviation from the mean (N=3).

Supplementary Figures: Statistical Analyses

All tables and figures were generated using JMP statistical software.

Analysis of Variance

Source	DF	Sum of Squares	Mean Square	F Ratio
Model	11	354.78574	32.2532	485.3519
Error	20	1.32907	0.0665	Prob > F
C. Total	31	356.11480		<.0001*

Parameter Estimates

Effect Tests

Source	Nparm	DF	Sum of Squares	F Ratio	Prob > F
MSM Strain	3	3	3.37936	16.9510	<.0001*
Treatment	2	2	341.57064	2570.004	<.0001*
Treatment*MSM Strain	6	6	8.83452	22.1572	<.0001*

Least Squares Means Plot

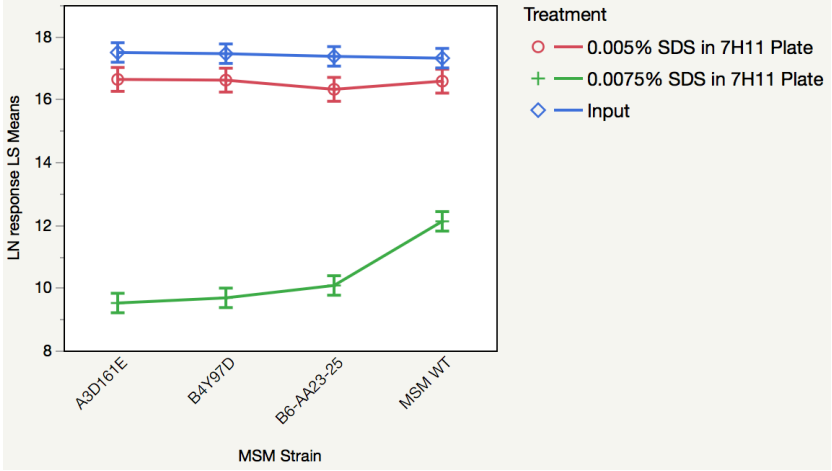

Level			Least Sq Mean
MSM WT	A		15.333261
B6-AA23-25		B	14.584828
B4Y97D		B	14.579532
A3D161E		B	14.545094

Levels not connected by same letter are significantly different.

Least Squares Means Table

Level	Least Sq Mean	Std Error	Mean
A3D161E	14.545094	0.09281336	14.2841
B4Y97D	14.579532	0.09281336	14.3258
B6-AA23-25	14.584828	0.09281336	14.3684
MSM WT	15.333261	0.09281336	15.1778

Least Squares Means Table

Level	Least Sq Mean	Std Error	Mean
0.005% SDS in 7H11 Plate	16.534100	0.09114091	16.5341
0.0075% SDS in 7H11 Plate	10.343666	0.07441625	10.3437
Input	17.404270	0.07441625	17.4043

Fig. S5. Two-way ANOVA for SDS stress response shown in Figure 7A. There was no statistically significant difference between Msm strains for input CFU counts, or growth response to 0.005% SDS. The difference in the growth response to 0.0075% SDS between WT and mutant strains was shown to be statistically significant (P< .0001) by a comparison of least squares means with a Tukey correction. Data were transformed into the natural log to fit the assumptions of the model of normally distributed residuals with constant variance.

Analysis of Variance

Source	DF	Sum of Squares	Mean Square	F Ratio
Model	14	110.27988	7.87713	39.6172
Error	30	5.96493	0.19883	Prob > F
C. Total	44	116.24482		<.0001*

Effect Tests

Source	Nparm	DF	Sum of Squares	F Ratio	Prob > F
Sample	4	4	1.02886	1.2936	0.2947
Treatment	2	2	107.20805	269.5957	<.0001*
Treatment*Sample	8	8	2.04298	1.2844	0.2885

Level			Least Sq Mean
Control	A		16.777901
Input	A		16.697798
SDS		B	13.464320

Levels not connected by same letter are significantly different.

Level		Least Sq Mean
A3D161E	A	15.921285
B6-AA23-25	A	15.657245
B4Y97D	A	15.631114
MSM WT	A	15.545048
WT in 8918	A	15.478673

Levels not connected by same letter are significantly different.

Least Squares Means Table

Level	Least Sq Mean	Std Error	Mean
A3D161E	15.921285	0.14863494	15.9213
B4Y97D	15.631114	0.14863494	15.6311
B6-AA23-25	15.657245	0.14863494	15.6572
MSM WT	15.545048	0.14863494	15.5450
WT in 8918	15.478673	0.14863494	15.4787

Least Squares Means Table

Level	Least Sq Mean	Std Error	Mean
Control	16.777901	0.11513213	16.7779
Input	16.697798	0.11513213	16.6978
SDS	13.464320	0.11513213	13.4643

Fig. S6: **Two-way ANOVA for SDS liquid stress test shown in Figure 7C.** Treatment with SDS was shown by a comparison of least squares means with a Tukey correction to have a statistically significant effect on growth (P< .0001). Differences in growth between strains were not statistically significant. Data were transformed into the natural log to fit the assumptions of the model of normally distributed residuals with constant variance.

Analysis of Variance

Source	DF	Sum of Squares	Mean Square	F Ratio
Model	5	97.576334	19.5153	540.3867
Error	12	0.433362	0.0361	Prob > F
C. Total	17	98.009696		<.0001*

Parameter Estimates

Effect Tests

Source	Nparm	DF	Sum of Squares	F Ratio	Prob > F
Sample	5	5	97.576334	540.3867	<.0001*

Level				Least Sq Mean
A3D161E EtBr	A			5.284271
B4Y97D EtBr	A			5.104847
MSM WT EtBr	A			4.926998
B6-AA23-25 EtBr	A			4.887696
EtBr Control		B		2.695511
MSM WT Control			C	-1.215402

Least Squares Means Table

Level	Least Sq Mean	Std Error	Mean
A3D161E EtBr	5.284271	0.10971709	5.2843
B4Y97D EtBr	5.104847	0.10971709	5.1048
B6-AA23-25 EtBr	4.887696	0.10971709	4.8877
EtBr Control	2.695511	0.10971709	2.6955
MSM WT Control	-1.215402	0.10971709	-1.2154
MSM WT EtBr	4.926998	0.10971709	4.9270

Fig. S7. One-way ANOVA for the ethidium bromide uptake assay shown in Figure 8. The difference in RFU between mutant and WT experimental strains was not statistically significant. The fluorescence of the control strains was shown by a comparison of least squares means with a Tukey correction to be statistically significant compared to that of the experimental strains. Data

were transformed into the natural log to fit the assumptions of the model of normally distributed residuals with constant variance.

Analysis of Variance

Source	DF	Sum of Squares	Mean Square	F Ratio
Model	39	26104278	669340	10.1101
Error	40	2648202	66205	Prob > F
C. Total	79	28752480		<.0001*

Parameter Estimates

Effect Tests

Source	Nparm	DF	Sum of Squares	F Ratio	Prob > F
Treatment 2	3	3	3907085	19.6716	<.0001*
Strain	9	9	12100074	20.3074	<.0001*
Treatment 2*Strain	27	27	10097118	5.6486	<.0001*

Least Squares Means Plot

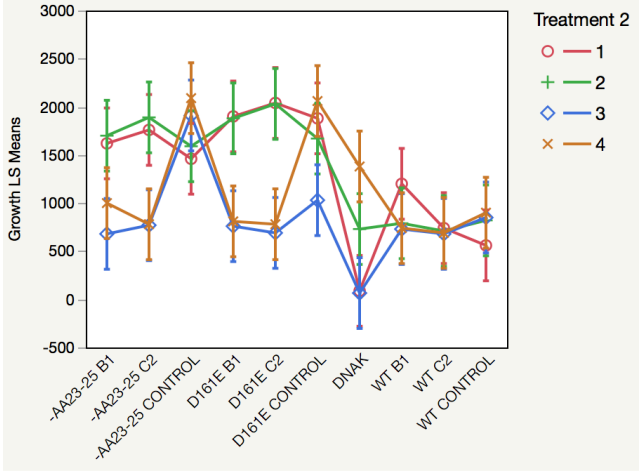

Least Squares Means Table

Level	Least Sq Mean	Std Error	Mean
-AA23-25 B1	1250.0000	90.970497	1250.00
-AA23-25 C2	1300.0000	90.970497	1300.00
-AA23-25 CONTROL	1762.5000	90.970497	1762.50
D161E B1	1337.5000	90.970497	1337.50
D161E C2	1385.0000	90.970497	1385.00
D161E CONTROL	1660.0000	90.970497	1660.00
DNAK	565.7500	90.970497	565.75
WT B1	865.0000	90.970497	865.00
WT C2	705.0000	90.970497	705.00
WT CONTROL	782.5000	90.970497	782.50

Least Squares Means Table

Level	Least Sq Mean	Std Error	Mean
1	1324.8000	57.534794	1324.80
2	1381.0000	57.534794	1381.00
3	816.5000	57.534794	816.50
4	1123.0000	57.534794	1123.00

Fig. S8. Two-way ANOVA for the ATc Synthetic Lethality Screening shown in Figure 9. Significant effects of both treatment and strain were found for the majority of samples. By F-test slicing, the growth response of the deletion mutant control to different treatments and the response of all WT strains to different treatments was shown to be not significant. Differences in the growth response within the –AA23-25 C2 strain, D161E B1 and C2 strains, and DnaK strain across treatment groups were statistically significant (P=0.0001). The difference in the growth response of the D161E control strain across treatments (P=0.0016) and of the –AA23-25 B1 strain across treatments (P=0.0005) was also significant. Significance was found by a comparison of least squares means with a Tukey correction. Treatment 1 consisted of a lack of pre-treatment with ATc, followed by plating on 7H11, Treatment 2 consisted of a lack of pre-treatment with ATc, followed by plating on 7H11 with ATc, Treatment 3 consisted of pre-treatment with ATc, followed by plating on 7H11, and Treatment 4 consisted of pre-treatment with ATc, followed by plating on 7H11 with ATc.